THE HONG KONG UNIVERSITY OF SCIENCE AND TECHNOLOGY

Final Report
for
Chemical Speciation of $PM_{2.5}$ Filter Samples

January 1 through December 31, 2017

(Quotation Ref. 16-02709)

Prepared by:

Prof. Jian Zhen Yu

Dr. Ting Zhang

Environmental Central Facility

The Hong Kong University of Science & Technology

Clear Water Bay, Kowloon, Hong Kong

Presented to:

Environmental Protection Department

The Government of the Hong Kong Special Administrative Region

May 2018

[This page was intentionally left blank.]

Table of Content

List of Figures

List of Tables

Acronyms, Abbreviations and Chemical Symbols

Ag	Silver	In	Indium
Al	Aluminum	Ir	Iridium
AQMS	Air Quality Monitoring Station	K	Potassium
AQO	Air Quality Objective	K^+	Potassium ion
AQRS	Air Quality Research Site	KC	Kwai Chung
As	Arsenic	La	Lanthanum
Au	Gold	LOD	Limit of Detection
Ba	Barium	LOQ	Limit of Quantification
BLK	Blank	Mg	Magnesium
Br	Bromine	MK	Mong Kok
Ca	Calcium	Mn	Manganese
Ca^{2+}	Calcium ion	Mo	Molybdenum
Cd	Cadmium	Na	Sodium
Cs	Cesium	Na^+	Sodium ion
CSN	Chemical Speciation Network	Nb	Niobium
Cu	Copper	NH_4^+	Ammonium
CW	Central/Western	NH_4NO_3	Ammonium nitrate
EC	Elemental carbon	$(NH_4)_2SO_4$	Ammonium sulfate
ED-XRF	Energy-Dispersive X-Ray Fluorescence Spectroscopy	NH_4HSO_4	Ammonium bisulfate
Eu	Europium	Ni	Nickel
Fe	Iron	NO_3^-	Nitrate
Ga	Gallium	O_2	Oxygen
He	Helium	OC	Organic carbon
Hf	Hafnium	P	Phosphorus
Hg	Mercury	Pb	Lead
HKENB	Hong Kong Environment Bureau	Pd	Palladium
HKEPD	Hong Kong Environmental Protection Department	PM	Particulate matter
HT	Hok Tsui		
IC	Ion chromatography		
IMPROVE_A	A thermal/optical carbon analysis temperature protocol		

$PM_{2.5}$	Particles with aerodynamic diameter ≤2.5 μm	TW	Tsuen Wan
QA	Quality assurance	U	Uranium
QC	Quality control	USEPA	United States Environmental Protection Agency
Rb	Rubidium	V	Vanadium
S	Sulfur	W	Wolfram
Sb	Antimony	WB	Clear Water Bay
Sc	Scandium	WHO	World Health Organization
Se	Selenium	Y	Yttrium
Si	Silicon	YL	Yuen Long
Sm	Samarium	Zn	Zinc
Sn	Tin	Zr	Zirconium
SO_4^{2-}	Sulfate		
Sr	Strontium		
Ta	Tantalum		
Tb	Terbium		
TC	Tung Chung		
Ti	Titanium		
Tl	Thallium		
TOR	Thermal Optical Reflectance		
TOT	Thermal Optical Transmittance		
TotC	Total carbon		

[This page was intentionally left blank.]

1. Introduction

1.1 Background

The Environmental Protection Department of the Hong Kong Special Administration Region (HKEPD) put in force an updated Air Quality Objectives (AQOs) in January 2014. In the new AQOs, the concentration limit for 24-hour average $PM_{2.5}$ is set to be 75 $\mu g/m^3$ with 9 exceedance days allowed while the limit for annual average $PM_{2.5}$ is 35 $\mu g/m^3$.

The Environment Bureau (ENB) and the HKEPD have been implementing a wide range of measures locally to reduce the air pollution. In November 2012, the Hong Kong Special Administrative Region and Guangdong Provincial Governments endorsed emission reduction targets for 2015 while in December 2017, the emission reduction targets for 2020 were set, strengthening the collaboration between Guangdong and Hong Kong to deal with the regional air pollution.

The on-going control measures aside, continuous monitoring of the air quality is necessary for the air pollution trend analysis. More specifically, the $PM_{2.5}$ chemical speciation studies would provide a better understanding on the nature and relative contributions of different emission sources that are responsible for the observed $PM_{2.5}$ levels in Hong Kong.

The HKEPD established a $PM_{2.5}$ chemical speciation network in 2000 and monitoring operations began in November 2000. Up to 2016, the HKEPD supported seven sampling sites which includes four collocated sites. In 2017, the network was reduced to five sampling sites with two collocated sites. HKUST has been supporting the HKEPD with the chemical speciation analysis of the $PM_{2.5}$ filter samples during 2011–2014 and in 2016 and 2017.

This report documents the $PM_{2.5}$ measurements and data validation for a twelve-month monitoring program from January to December 2017. The data were analyzed to characterize the composition and temporal and spatial variations of $PM_{2.5}$ concentrations in Hong Kong. Trends of $PM_{2.5}$ concentration and chemical composition were established by comparing the current study to the previous 12-month $PM_{2.5}$ studies since 2000. The monitoring data can further be used to explore the source contributions and investigate hypotheses regarding the formation of $PM_{2.5}$ episodes.

1.2 Project Objectives and Task Description

The Environmental Central Facility (ENVF) at the Hong Kong University of Science and Technology (HKUST) has been contracted by the HKEPD in the analysis of $PM_{2.5}$ samples acquired over the course from January to December 2017. The objectives of this study were to:

- Determine the organic and inorganic composition of $PM_{2.5}$ and how it differs by season and proximity to different types of emission sources.
- Based on the ambient concentrations of certain tracer compounds, determine the contributions of different sources to $PM_{2.5}$ in Hong Kong.
- Investigate and understand the influences of meteorological/atmospheric conditions on $PM_{2.5}$ episodic events in Hong Kong.
- Establish inter-annual variability of $PM_{2.5}$ concentration and chemical composition in Hong Kong urban and rural areas.

The ENVF/HKUST team is responsible for:

- Receiving samples from the HKEPD and analyzing the filter samples for gravimetric mass and for an array of chemical constituents, including elements, soluble anions and cations, and carbonaceous material.
- Assembling validated sets of data from the analyses and preparing data files, which will be entered into the HKEPD $PM_{2.5}$ speciation database.

1.3 Technical Approach

During the sampling period from January to December 2017, 24-hour $PM_{2.5}$ filter samples were acquired once every six days from the roadside-source-dominated Mong Kok (MK) Air Quality Monitoring Station (AQMS), the urban Tsuen Wan (TW) and Kwai Chung (KC) AQMSs, the new town Yuen Long (YL) AQMS, and the suburban Clear Water Bay (WB) Air Quality Research Site (AQRS) which is located on the campus of the Hong Kong University of Science and Technology. Three Partisol samplers (Rupprecht & Patachnick, Model 2025, Albany, NY, USA) were used at MK and WB sites, two BGI PQ200 samplers were placed at TW and YL (BGI Incorporated, Model PQ200, Butler, NJ, USA), and two Partisol samplers were deployed at KC sites to obtain $PM_{2.5}$ samples on both Teflon-membrane and quartz fiber 47-mm filters. All sampled Teflon-membrane and quartz fiber filters were analyzed for mass by gravimetric analysis by HKEPD's contractor and then subjected to a suite of chemical analyses, including 1) determination of elements for atomic number ranging from 11 (sodium) to 92 (uranium) using Energy-Dispersive X-Ray Fluorescence (ED-XRF) Spectroscopy; 2) determination of chloride, nitrate, sulfate, sodium, ammonium, and potassium using Ion Chromatography (IC); and 3) determination of organic carbon (OC), elemental carbon (EC), total carbon (TotalC) and individual thermal fractions for OC, EC, and pyrolyzed carbon on quartz fiber filters using Thermal Optical Transmittance (TOT) and Thermal Optical Reflectance (TOR) methods coupled with IMPROVE_A protocol.

2. Sampling Network

2.1 Ambient $PM_{2.5}$ Monitoring Network

24-hour $PM_{2.5}$ filter samples were collected at four AQMSs and one AQRS in Hong Kong once every six days from January to December 2017. The five sampling sites are shown in Figure 1, representing roadside (MK), urban (TW and KC), new town (YL), and suburban (WB) areas. The names, codes, locations, and descriptions of the individual sites are listed in Table 1.

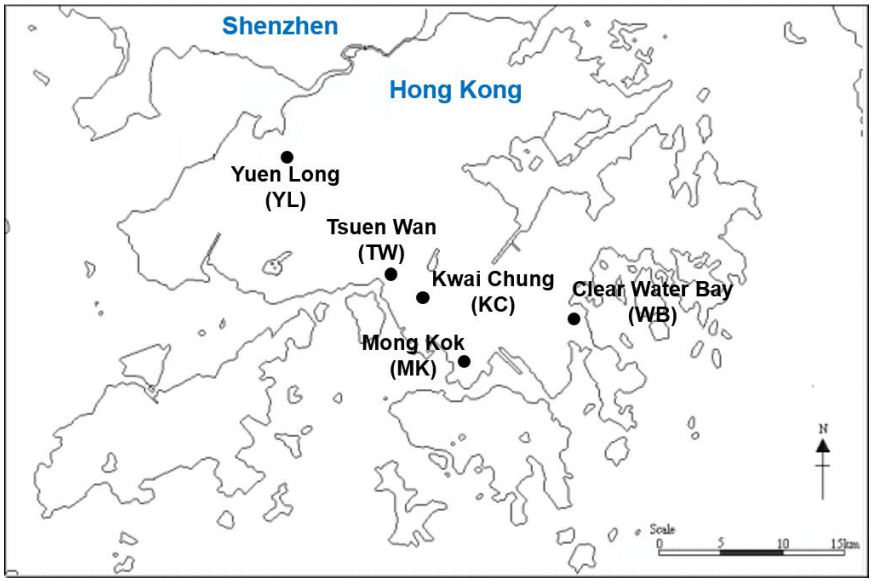

Figure 1. Monitoring sites in Hong Kong $PM_{2.5}$ speciation network in 2017.

Table 1. Descriptions of the monitoring sites.

Site Name	Site Code	Site Location	Site Description
Mong Kok	MK	Junction of Lai Chi Kok Road and Nathan Road, Kowloon	Urban roadside in mixed residential/commercial area with heavy traffic and surrounded by many tall buildings
Clear Water Bay	WB	Rooftop of a pump house next to Coastal Marine Lab, HKUST Campus, Clear Water Bay	Clean rural area with little residential and commercial development on the east coast of Sai Kung
Tsuen Wan	TW	Rooftop of Princess Alexandra Community Center, 60 Tai Ho Road, New Territories	Urban, densely populated, residential site with mixed commercial and industrial developments. Located northwest of the MK site
Yuen Long	YL	Rooftop of Yuen Long District Branch Office Building, 269 Castle Peak Road, New Territories	Residential town, about 15 km southwest of Shenzhen
Kwai Chung	KC	Rooftop of the Kwai Chung Police Station, 999 Kwai Chung Road	Urban, densely populated residential site with mixed commercial and industrial developments, close to the Kwai Tsing Container Terminals

2.2 Ambient $PM_{2.5}$ Measurements

A total of 12 samplers were employed to obtain $PM_{2.5}$ samples around Hong Kong. The detailed arrangement of the samplers is described in Table 2.

Table 2. Arrangement of the air samplers in the monitoring sites.

Location	Sampler Brand	No. of Samplers	Collocated Samples
MK AQMS	Partisol®	3	Teflon Filters
WB AQRS	Partisol®	3	Quartz Fiber Filters
TW AQMS	BGI PQ200	2	
YL AQMS	BGI PQ200	2	
KC AQMS	Partisol®	2	

Each air sampler was equipped with an $PM_{2.5}$ inlet with Very Sharp Cut Cyclone. The samplings were conducted at a flow rate of 16.7 L/min. At this flow rate, a nominal volume of approx. 24.0 m^3 of ambient air would be sampled over a 24-hour period. The air samplers were configured to take either a Teflon-membrane filter or a quartz fiber filter. For this study, the following filters were chosen: 1) Whatman (Clifton, NJ, USA), $PM_{2.5}$ membrane, PTFE, 46.2 mm with support ring (#7592204); and 2) Pall Life Sciences (Ann Arbor, MI, USA), 2500QAT-UP, 47 mm, Tissuquartz^{TM} filters (#7202).

The air samplers were operated and maintained by HKEPD's contractor, AECOM Asia Company Limited, throughout the study period. The ENVF/HKUST team was responsible for pre- and post-sampling procedures required for quality assurance and sample preservation. ENVF/HKUST team was also responsible for the gravimetric analysis on both filter types before and after sampling.

The collected Teflon-membrane filters were used for gravimetric analysis for $PM_{2.5}$ mass concentrations and elemental analysis (for more than 40 elements with atomic number ranging from 11 to 92) by ED-XRF [Watson et al., 1999]. The collected quartz fiber filters were analyzed for mass concentrations by gravimetry, for carbon contents by multiple thermal optical methods, and for chloride (Cl^-), nitrate (NO_3^-), sulfate (SO_4^{2-}), water-soluble sodium (Na^+), ammonium (NH_4^+), and water-soluble potassium (K^+) by IC.

A major uncertainty in determining carbon concentrations lies in the differentiation of organic and elemental carbon during analysis. EC has been defined as the carbon that evolves after the detected optical signal attains the value it had prior to commencement of heating and the rest of the carbon is considered to be OC [Chow et al., 1993; Birch and Cary, 1996]. The split of OC and EC in the thermal analysis depends on several parameters including temperature setpoints, temperature ramping rates, residence time at each setpoint, combustion atmospheres, and optical signal used. Heating in an inert atmosphere causes certain OC to pyrolyze or char, inflating the EC in the sample. The extent of pyrolysis is dependent on thermal/temperature protocols. A laser is used to correct for pyrolitically-produced EC by monitoring changes in filter darkness during the thermal evolution process by detecting either filter transmittance (thermal/optical transmittance [TOT] method) or reflectance (thermal/optical reflectance [TOR] method). However, this introduces another problem related to inner/near-surface filter pyrolysis. It is found that pyrolysis occurs both within filter and on the filter surface. TOT

method measures light transmittance which goes through the filter and is more likely influenced by the inner filter char while TOR method is more influenced by the charring of near-surface deposit. Results obtained with the two methods are compared and evaluated in Section 3.3.4.

2.3 Sample Delivery and Filter Conditions

A total of 792 filter samples including 396 Teflon filters and 396 quartz fiber filters were received. The valid sampling dates are summarized in Table 3. In 2017, there were 60 valid sampling events at MK, WB, TW, and KC sites, and 59 at YL site.

Table 3. Valid sampling dates for the $PM_{2.5}$ samples in 2017 (Quotation Ref. 16-02709).

Sampling Dates					
January 2017	February 2017	March 2017	April 2017	May 2017	June 2017
170109BLK	170202	170304	170403	170503	170602
170115	170208	170310 w/BLK	170409	170509BLK	170608
170117	170214	170316	170415	170515	170614
170121	170220	170322	170427	170521	170626
170127	170226	170328	170429	170524	170628
				170527	
July 2017	August 2017	September 2017	October 2017	November 2017	December 2017
170702	170801	170906	171006	171105	171205
170708 w/BLK	170807	170912 w/BLK	171012	171111 w/BLK	171211
170714	170815	170918	171018	171117	171217
170720	170819	170924	171024	171123	171221
170726	170825	170930	171030	171129	171227
	170831				

During the Level I data validation, 1 filter sample was identified to be invalid. The corresponding sample ID, filter ID, and a brief account for invalidating the sample are provided in Table 4.

Table 4. Invalid $PM_{2.5}$ filter sample identified during field validation in 2017 (Quotation Ref. 16-02709).

Sample ID	Filter ID	Cause	Remarks
YL171211SF01Q	Q0010408	Sampler failure	N/A

For this sampling date at YL site, the chemical information was incomplete since only one Teflon fiber sample was collected and no valid quartz filter sample was available at this site in this sampling event.

3. Database and Data Validation

3.1 Data File Preparation

An electronic database for the analytical results is established for Hong Kong $PM_{2.5}$ data archive. Detailed data processing and data validation are documented in Section 3.3. The data are available on Compact Disc in the format of Microsoft Excel spreadsheets for convenient distribution to data users. The contents of the final data files are summarized in Table 5.

Table 5. Summary of data files for the 2017 $PM_{2.5}$ study (EPD Quotation Ref. 16-02709) in Hong Kong.

Category	Database File	File Description
I. DATABASE DOCUMENTATION		
	16-02709_ID.xls	Defines the field sample names, measurement units, and formats used in the database file
II. MASS AND CHEMICAL DATA		
	16-02709_PM2.5.xls	Contains $PM_{2.5}$ mass data and chemical data for samples collected by $PM_{2.5}$ air samplers at five sites once every six days in 2017
III. DATABASE VALIDATION		
	16-02709_FLAG.xls	Contains both field sampling and chemical analysis data validation flags

3.2 Measurement and Analytical Specifications

The measurement/analysis methods are described in Section 1.3 and every measurement consists of 1) a value; 2) a precision (uncertainty), and 3) a validity statement. The values are obtained by different analysis methods. The precisions are estimated through standard testing, blank analysis, and replicate analysis. The validity of each measurement is indicated by appropriate flagging in the database, while the validity of chemical analysis results are evaluated by data validations described in Section 3.3.

A total of 60 sets of ambient $PM_{2.5}$ samples and 6 sets of field blanks were received during this study. Collocated sampling was conducted at 2 out of 5 sites and the collocated samples were used for data validation purpose. Of the 792 $PM_{2.5}$ filter samples received, 791 filter samples are considered valid after Level I data validation. Therefore, a total of 791 filters (719 $PM_{2.5}$ samples and 72 field blanks) were submitted for comprehensive chemical analyses.

3.2.1 Precision Calculations and Error Propagation

Measurement precisions are propagated from precisions of volumetric measurements, chemical composition measurements, and field blank variability using the methods of Bevington [1969] and Watson et al. [2001]. The following equations are used to calculate the prevision associated with filter-based measurements:

$$C_i = \frac{M_i - B_i}{V} \quad (1)$$

$$V = Q \times T \quad (2)$$

$$B_i = \frac{1}{n}\sum_{j=1}^{n} B_{ij} \qquad for\ B_i > \sigma_{B_i} \quad (3)$$

$$B_i = 0 \qquad for\ B_i \leq \sigma_{B_i} \quad (4)$$

$$\sigma_{B_i} = STD_{B_i} = \left[\frac{1}{n-1}\sum_{j=1}^{n}\left(B_{ij} - B_i\right)^2\right]^{\frac{1}{2}} \qquad for\ STD_{B_i} > SIG_{B_i} \quad (5)$$

$$\sigma_{B_i} = SIG_{B_i} = \left[\frac{1}{n}\sum_{j=1}^{n}\left(\sigma_{B_{ij}}\right)^2\right]^{\frac{1}{2}} \qquad for\ STD_{B_i} \leq SIG_{B_i} \quad (6)$$

$$\frac{\sigma_V}{V} = 0.05 \quad (7)$$

$$\sigma_{C_i} = \left[\frac{\sigma_{Mi}^2 + \sigma_{Bi}^2}{V^2} + \frac{\sigma_V^2 (M_i - B_i)^2}{V^4}\right]^{\frac{1}{2}} \quad (8)$$

Where:

B_i = average amount of species i on field blanks

B_{ij} = the amount of species i found on field blank j

C_i = the ambient concentration of species i

Q = flow rate throughout sampling period

M_i = amount of species i on the substrate

n = total number of samples in the sum

SIG_{Bi} = the root mean square error (RMSE), the square root of the averaged sum of the squared σ_{Bij}

STD_{Bi} = standard deviation of the blank

σ_{Bi} = blank precision for species i

σ_{Bij} = precision of the species i found on field blank j

σ_{Ci} = propagated precision for the concentration of species i

σ_{Mi} = precision of amount of species i on the substrate

σ_V = precision of sample volume

T = sample duration

V = volume of air sampled

The uncertainty of the measured value and the average uncertainty of the field blanks for each species are used to propagate the overall precision for each blank subtracted concentration value. The final value is propagated by taking the square root of the sum of the squares of the calculated uncertainty and the average field blank uncertainty for each measurement.

3.2.2 Analytical Specifications

The precisions (σ_{Mi}) were determined from duplicate analysis of samples. When duplicate sample analysis is made, the range of results, R, is nearly as efficient as the standard deviation since two measures differ by a constant ($1.128\sigma_{Mi} = R$).

Table 6. Field blank concentrations of $PM_{2.5}$ samples collected at MK, WB, TW, YL, and KC sites during the study period (2017) in Hong Kong.

	Amount on µg/47-mm filter					
Species	**Total No. of Blanks**	**Field Blank Std. Dev. (STD_{Bi})**	**Root Mean Squared Blank Precision (SIG_{Bi})**	**Blank Precision (σ_{Bi})**	**Average Field Blank**	**Blank Subtracted (B_i)**
Na^+	36	0.121	0.594	0.594	0.349	0.000
NH_4^+	36	0.540	0.695	0.695	-0.180	0.000
K^+	36	0.099	1.456	1.456	0.127	0.000
Cl^-	36	0.098	0.409	0.409	0.958	0.958
NO_3^-	36	0.490	1.560	1.560	3.746	3.746
SO_4^{2-}	36	1.775	9.739	9.739	4.343	0.000
OC1	36	1.027	3.955	3.955	4.012	4.012
OC2	36	0.710	3.143	3.143	4.523	4.523
OC3	36	1.538	4.162	4.162	6.494	6.494
OC4	36	0.607	2.171	2.171	1.552	0.000
EC1	36	0.503	2.868	2.868	0.420	0.000
EC2	36	0.663	1.963	1.963	1.473	0.000
EC3	36	0.590	2.037	2.037	1.227	0.000

Species	Amount on µg/47-mm filter					
	Total No. of Blanks	**Field Blank Std. Dev. (STD_{Bi})**	**Root Mean Squared Blank Precision (SIG_{Bi})**	**Blank Precision (σ_{Bi})**	**Average Field Blank**	**Blank Subtracted (B_i)**
PyC_TOR	36	0.665	1.640	1.640	-0.175	0.000
OC_TOR	36	3.156	11.156	11.156	16.406	16.406
EC_TOR	36	1.742	5.216	5.216	3.295	0.000
TotC	36	4.497	16.012	16.012	19.701	19.701
PyC_TOT	36	1.579	2.535	2.535	1.593	0.000
OC_TOT	36	4.376	11.361	11.361	18.174	18.174
EC_TOT	36	1.649	5.029	5.029	1.527	0.000
Na	36	0.118	0.300	0.300	-0.018	0.000
Mg	36	0.221	0.228	0.228	-0.275	0.000
Al	36	0.152	0.259	0.259	0.022	0.000
Si	36	0.337	0.880	0.880	0.173	0.000
P	36	0.023	0.077	0.077	-0.002	0.000
S	36	0.039	0.228	0.228	0.011	0.000
Cl	36	0.129	0.197	0.197	0.055	0.000
K	36	0.030	0.030	0.030	0.008	0.000
Ca	36	0.221	0.514	0.514	0.105	0.000
Sc	36	0.129	0.177	0.177	-0.021	0.000
Ti	36	0.005	0.052	0.052	0.002	0.000
V	36	0.007	0.016	0.016	0.007	0.000
Cr	36	0.039	0.078	0.078	0.055	0.000
Mn	36	0.045	0.155	0.155	0.016	0.000
Fe	36	0.186	0.281	0.281	0.166	0.000
Co	36	0.009	0.020	0.020	-0.009	0.000
Ni	36	0.014	0.029	0.029	-0.004	0.000
Cu	36	0.018	0.048	0.048	0.017	0.000
Zn	36	0.017	0.048	0.048	0.033	0.000
Ga	36	0.027	0.077	0.077	0.031	0.000
Ge	36	0.056	0.205	0.205	0.022	0.000
As	36	0.000	0.121	0.121	0.000	0.000
Se	36	0.000	0.121	0.121	0.000	0.000
Br	36	0.021	0.044	0.044	0.007	0.000
Rb	36	0.015	0.043	0.043	0.012	0.000

Species	Amount on µg/47-mm filter					
	Total No. of Blanks	**Field Blank Std. Dev. (STD_{Bi})**	**Root Mean Squared Blank Precision (SIG_{Bi})**	**Blank Precision (σ_{Bi})**	**Average Field Blank**	**Blank Subtracted (B_i)**
Sr	36	0.017	0.048	0.048	-0.015	0.000
Y	36	0.014	0.030	0.030	-0.037	0.000
Zr	36	0.039	0.104	0.104	0.042	0.000
Nb	36	0.038	0.104	0.104	-0.029	0.000
Mo	36	0.034	0.061	0.061	-0.069	0.000
Rh	36	0.044	0.114	0.114	-0.089	0.000
Pd	36	0.058	0.140	0.140	-0.046	0.000
Ag	36	0.046	0.117	0.117	-0.002	0.000
Cd	36	0.050	0.127	0.127	0.010	0.000
In	36	0.073	0.128	0.128	0.020	0.000
Sn	36	0.074	0.200	0.200	-0.060	0.000
Sb	36	0.080	0.217	0.217	-0.032	0.000
Te	36	0.127	0.332	0.332	0.225	0.000
I	36	0.119	0.325	0.325	-0.082	0.000
Cs	36	0.328	0.762	0.762	0.331	0.000
Ba	36	0.336	0.697	0.697	0.148	0.000
La	36	0.519	0.835	0.835	-0.022	0.000
Ce	36	0.014	0.047	0.047	0.007	0.000
Sm	36	0.034	0.073	0.073	0.002	0.000
Eu	36	0.081	0.218	0.218	0.036	0.000
Tb	36	0.016	0.028	0.028	0.008	0.000
Hf	36	0.171	0.382	0.382	0.151	0.000
Ta	36	0.026	0.297	0.297	0.005	0.000
W	36	0.268	0.751	0.751	-0.107	0.000
Ir	36	0.033	0.107	0.107	-0.008	0.000
Au	36	0.018	0.097	0.097	0.006	0.000
Hg	36	0.000	0.096	0.096	0.000	0.000
Tl	36	0.032	0.082	0.082	-0.012	0.000
Pb	36	0.043	0.096	0.096	-0.020	0.000
U	36	0.049	0.153	0.153	-0.002	0.000

The analytical specifications for the 24-hour $PM_{2.5}$ measurements obtained during the study are summarized in Table 7. Limits of detection (LOD) and limits of quantitation (LOQ) are given. The LOD of an analyte may be described as that concentration which gives an instrument signal significantly different from the "blank" or "background" signal. In this study LOD is defined as the concentration at which instrument response equals three times the standard deviation of the concentrations of low level standards. As a further limit, the LOQ is regarded as the lower limit for precise quantitative measurements and is defined as a concentration corresponding to ten times the standard deviation of the concentrations of low level standards. The LOQs should always be equal to or larger than the analytical LODs and it was the case for all the chemical species listed in Table 7. Both the LODs and LOQs are in the unit of $\mu g/m^3$ assuming the effective sampling area of the 47-mm filter is 11.98 cm^2 and the sampling volume is 24 m^3.

Table 7. Analytical specifications of 24-hour $PM_{2.5}$ measurements at MK, WB, TW, YL, and KC sites during the study period (2017) in Hong Kong.

Species	Analytical Method	LOD, $\mu g/m^3$	LOQ, $\mu g/m^3$	No. of Valid Values	No. > LOD	% > LOD	No. > LOQ	% > LOQ
Na^+	IC	0.025	0.082	359	359	100%	338	94%
NH_4^+	IC	0.029	0.096	359	359	100%	359	100%
K^+	IC	0.061	0.202	359	307	86%	171	48%
Cl^-	IC	0.017	0.056	359	269	75%	150	42%
NO_3^-	IC	0.064	0.213	359	316	88%	229	64%
SO_4^{2-}	IC	0.405	1.352	359	359	100%	356	99%
OC1	TOR	0.035	0.118	359	323	90%	323	90%
OC2	TOR	0.058	0.195	359	359	100%	359	100%
OC3	TOR	0.074	0.246	359	359	100%	359	100%
OC4	TOR	0.043	0.145	359	359	100%	359	100%
EC1	TOR	0.061	0.205	359	357	99%	353	98%
EC2	TOR	0.039	0.131	359	357	99%	346	96%
EC3	TOR	0.038	0.127	359	111	31%	15	4%
PyC_TOR	TOR	0.036	0.122	359	320	89%	313	87%
OC_TOR	TOR	0.202	0.674	359	359	100%	359	100%
EC_TOR	TOR	0.106	0.353	359	358	100%	351	98%
TotC	TOR	0.302	1.006	359	359	100%	359	100%
PyC_TOT	TOT	0.051	0.169	359	352	98%	348	97%
OC_TOT	TOT	0.202	0.674	359	359	100%	359	100%
EC_TOT	TOT	0.106	0.353	359	357	99%	346	96%
Na	XRF	0.012	0.041	360	360	100%	360	100%
Mg	XRF	0.015	0.051	360	360	100%	329	91%

Species	Analytical Method	LOD, µg/m^3	LOQ, µg/m^3	No. of Valid Values	No. > LOD	% > LOD	No. > LOQ	% > LOQ
Al	XRF	0.010	0.034	360	359	100%	327	91%
Si	XRF	0.035	0.115	360	345	96%	261	73%
P	XRF	0.003	0.011	360	152	42%	25	7%
S	XRF	0.009	0.031	360	360	100%	360	100%
Cl	XRF	0.008	0.026	360	331	92%	241	67%
K	XRF	0.001	0.004	360	360	100%	360	100%
Ca	XRF	0.020	0.068	360	358	99%	258	72%
Sc	XRF	0.007	0.025	360	0	0%	0	0%
Ti	XRF	0.002	0.007	360	332	92%	205	57%
V	XRF	0.001	0.002	360	355	99%	333	93%
Cr	XRF	0.003	0.010	360	156	43%	7	2%
Mn	XRF	0.006	0.021	360	240	67%	42	12%
Fe	XRF	0.010	0.034	360	357	99%	352	98%
Co	XRF	0.001	0.003	360	29	8%	1	0%
Ni	XRF	0.001	0.004	360	327	91%	136	38%
Cu	XRF	0.002	0.006	360	358	99%	304	84%
Zn	XRF	0.002	0.006	360	360	100%	358	99%
Ga	XRF	0.003	0.009	360	17	5%	0	0%
Ge	XRF	0.008	0.028	360	12	3%	0	0%
As	XRF	0.005	0.017	360	26	7%	0	0%
Se	XRF	0.005	0.017	360	0	0%	0	0%
Br	XRF	0.002	0.006	360	320	89%	205	57%
Rb	XRF	0.002	0.005	360	69	19%	1	0%
Sr	XRF	0.002	0.007	360	78	22%	2	1%
Y	XRF	0.002	0.005	360	0	0%	0	0%
Zr	XRF	0.004	0.013	360	66	18%	0	0%
Nb	XRF	0.005	0.015	360	0	0%	0	0%
Mo	XRF	0.003	0.011	360	0	0%	0	0%
Rh	XRF	0.006	0.019	360	0	0%	0	0%
Pd	XRF	0.006	0.021	360	0	0%	0	0%
Ag	XRF	0.005	0.016	360	9	3%	0	0%
Cd	XRF	0.005	0.017	360	13	4%	0	0%
In	XRF	0.005	0.017	360	35	10%	0	0%
Sn	XRF	0.009	0.030	360	63	18%	0	0%
Sb	XRF	0.009	0.031	360	12	3%	0	0%

Species	Analytical Method	LOD, µg/m^3	LOQ, µg/m^3	No. of Valid Values	No. > LOD	% > LOD	No. > LOQ	% > LOQ
Te	XRF	0.010	0.034	360	121	34%	0	0%
I	XRF	0.016	0.054	360	1	0%	0	0%
Cs	XRF	0.021	0.071	360	112	31%	0	0%
Ba	XRF	0.024	0.080	360	109	30%	0	0%
La	XRF	0.032	0.108	360	17	5%	0	0%
Ce	XRF	0.002	0.006	360	23	6%	0	0%
Sm	XRF	0.003	0.010	360	94	26%	0	0%
Eu	XRF	0.009	0.029	360	31	9%	0	0%
Tb	XRF	0.001	0.004	360	39	11%	24	7%
Hf	XRF	0.015	0.049	360	17	5%	0	0%
Ta	XRF	0.012	0.041	360	47	13%	0	0%
W	XRF	0.032	0.107	360	0	0%	0	0%
Ir	XRF	0.005	0.015	360	0	0%	0	0%
Au	XRF	0.004	0.013	360	1	0%	0	0%
Hg	XRF	0.004	0.013	360	0	0%	0	0%
Tl	XRF	0.003	0.012	360	0	0%	0	0%
Pb	XRF	0.004	0.014	360	244	68%	184	51%
U	XRF	0.006	0.021	360	4	1%	0	0%

The number of reported concentrations for each species and number of reported concentrations greater than the LODs and LOQs are also summarized in Table 7. For the 359 valid quartz fiber filter samples and 360 valid Teflon filter samples, major ions (including sulfate, ammonium, and water-soluble sodium), organic carbon, elemental carbon, sodium (Na), magnesium (Mg), aluminum (Al), silicon (Si), sulfur (S), potassium (K), calcium (Ca), titanium (Ti), vanadium (V), iron (Fe), nickel (Ni), copper (Cu) and zinc (Zn) were detected (>LOD) in almost all the samples (more than 90%). A number of transition metals (e.g. Sc, Co, Ga, Ge, As, Se, Y, Nb, Mo, Rh, Pd, Ag, Cd, In, Sb, La, Ce, Eu, Hf, Ta, W, Ir, Au, Hg, Tl, and U) were not detected in most of the samples (less than 15%). Species from motor vehicle exhaust such as Br and Pb were detected in 89% and 68% of the samples, respectively. V and Ni, which are residual-oil-related species, were both detected in most of the samples. This is typical for urban and suburban sites in most regions. Toxic species emitted from industrial sources, such as Cd and Hg, were not detected (4% and 0% of the samples, respectively). Soil/dust-related species, including Al, Si, Ca, Ti, and Fe, were found above the LODs in more than 92% of the samples and above the LOQs in more than 57% of the samples.

In general, the analytical specifications shown in Table 7 suggest that the $PM_{2.5}$ samples collected during the study period possess adequate loadings for chemical analysis. The detection limits of the selected analytical methods were sufficiently low to establish valid measurements with acceptable precision.

3.3 Data Validation

Three levels of data validation were conducted to the data set acquired from the study.

Level I data validation: 1) flag measurements for deviations from procedures; 2) identify and remove invalid values and indicate the reasons for invalid sampling, and 3) estimate precisions from replicate and blank analyses.

Level II data validation examines internal consistency tests among different data and attempts to resolve discrepancies based on known physical relationships between variables: 1) compare a sum of chemical species to mass concentrations; 2) compare measurements from different methods; 3) compare collocated measurements; 4) examine time series from different sites to identify and investigate outliers, and 5) prepare a data qualification statement.

Level III data validation is part of the data interpretation process and should identify unusual values including: 1) extreme values; 2) values which would otherwise normally track the values of other variables in a time series, and 3) values for observables which would normally follow a qualitatively predictable spatial or temporal pattern. External consistency tests are used to identify values in the data set which appear atypical when compared to other data sets. The first assumption upon finding a measurement which is inconsistent with physical expectations is that the unusual value is due to a measurement error. If nothing unusual is found upon tracing the path of the measurement, the value would be assumed to be a valid result of an environmental cause.

Level I data validation was performed and the validation flags and comments are stated in the database as documented in Section 3.1. Level II validation tests and results are described in the following subsections including 1) sum of chemical species versus $PM_{2.5}$ mass; 2) physical and chemical consistency; 3) anion/cation balance; 4) carbon measurements by different thermal/optical methods; 5) reconstructed versus measured mass, and 6) collocated measurement comparison. For Level III data validation, parallel consistency tests were applied to data sets from the same population (e.g., region, period of time) by different data analysis approaches. Collocated samples collected at two out of the five sampling sites were examined. Comparison of $PM_{2.5}$ mass concentrations obtained from gravimetric analysis and from 24-hr average continuous measurements were also conducted. The Level III data validation continues for as long as the database is maintained. For Level II/III data validation in this study, correlations and linear regression statistics were performed on the valid data set and scatter plots were generated for better comparison.

3.3.1 Sum of Chemical Species versus $PM_{2.5}$ Mass

The sum of the individual chemical concentrations determined in this study for $PM_{2.5}$ samples should be less than or equal to the corresponding mass concentrations obtained from gravimetric measurements. The chemical species include those that were quantified on both Teflon-membrane filters and quartz fiber filters. To avoid double counting, chloride (Cl^-), total potassium (K), soluble sodium (Na^+), and sulfate (SO_4^{2-}) are included in the sum while total sulfur (S), total chlorine (Cl), total sodium (Na), and soluble potassium (K^+) are excluded. Carbon concentration is represented by the sum of organic carbon and elemental carbon. Unmeasured ions, metal oxides, or hydrogen and oxygen associated with organic carbon are not counted into the measured concentrations.

The sum of chemical species was plotted against the measured $PM_{2.5}$ mass on Teflon filters for each of the individual sites in Figure 2. Linear regression analysis results and the average ratios of Y over X are both shown in Table 8 for comparison. Each plot contains a solid line indicating the slope with intercept and a dashed 1:1 line. Measurement uncertainties associated with the x- and y-axes are shown and the uncertainties of the $PM_{2.5}$ mass data were assumed to be 5% of the concentrations.

A strong correlation (R^2 = 0.98) was found between the sum of measured species and mass with a slope of 0.78±0.006.

Limits used for identifying reconstructed mass outliers are referring to those in Speciation Trends Network program suggested by USEPA [2012] and are listed as follows,

Lower Limit: [Sum of Chemical Species]/[Measured Mass] = 0.60

Upper Limit: [Sum of Chemical Species]/[Measured Mass] = 1.32

Based on these criteria, no sample was flagged as an outlier. It is noted that this test is helpful for sites with appreciable filter loadings and has been found less useful for lower level filter loading [RTI, 2005].

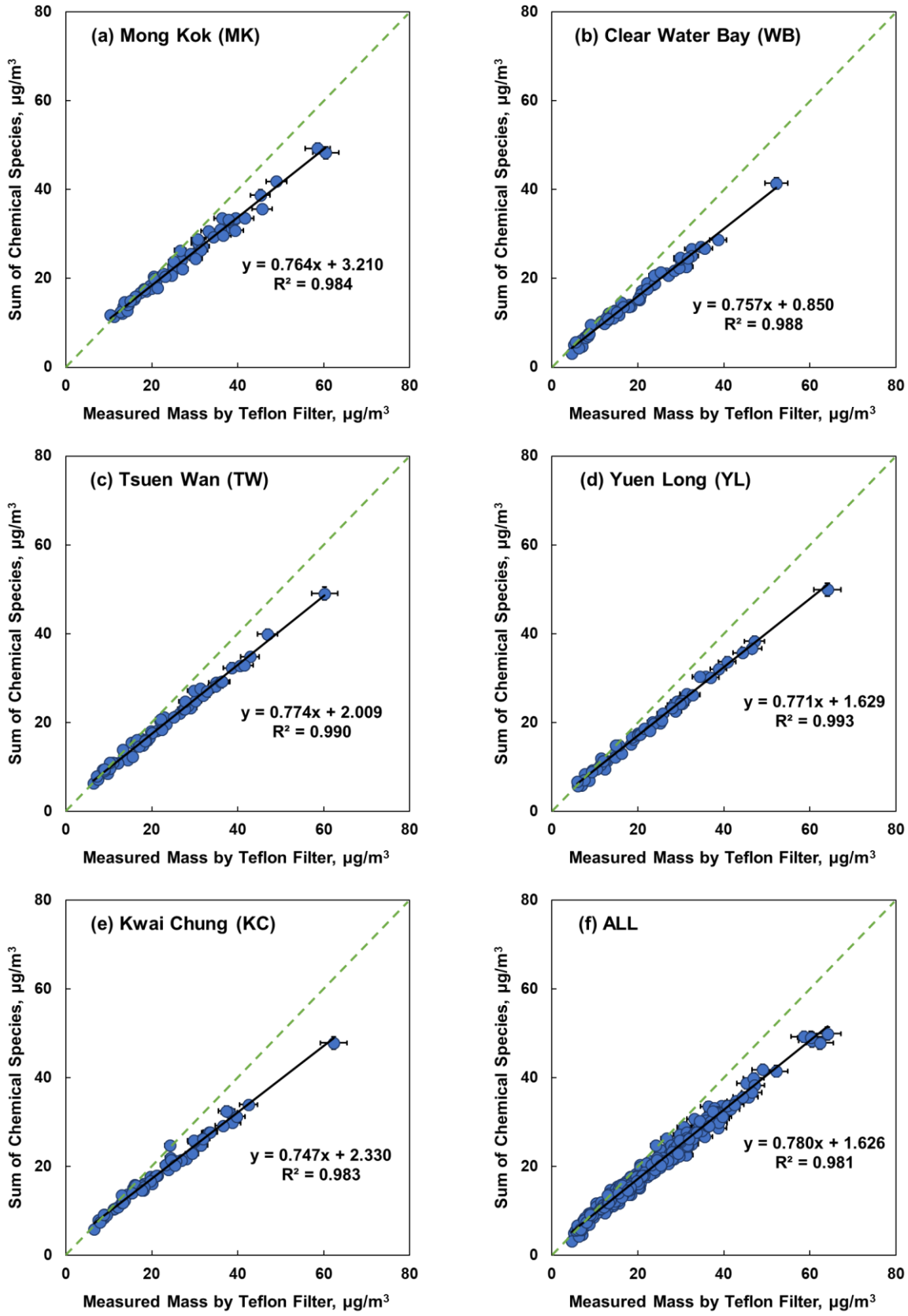

Figure 2. Scatter plots of sum of measured chemical species versus measured mass on Teflon filter for $PM_{2.5}$ samples collected at (a) MK, (b) WB, (c) TW, (d) YL, (e) KC, and (f) ALL.

Table 8. Statistics analysis of sum of measured chemical species versus measured mass on Teflon filters for $PM_{2.5}$ samples collected in this study (Quotation Ref. 16-02709).

Statistics/Site	MK	WB	TW	YL	KC	ALL
n	60	60	60	59	60	299
Slope	0.764 (±0.013)	0.757 (±0.011)	0.774 (±0.010)	0.771 (±0.009)	0.747 (±0.013)	0.780 (±0.006)
Intercept	3.210 (±0.380)	0.850 (±0.235)	2.009 (±0.258)	1.629 (±0.219)	2.330 (±0.312)	1.626 (±0.158)
R^2	0.984	0.988	0.990	0.993	0.983	0.981
AVG mass	27.18	18.67	22.38	22.50	22.08	22.56
AVG sum	23.98	14.98	19.33	18.97	18.81	19.22
AVG sum/mass	0.905 (±0.073)	0.817 (±0.075)	0.891 (±0.080)	0.868 (±0.077)	0.876 (±0.073)	0.872 (±0.081)

3.3.2 Physical and Chemical Consistency

Measurements of chemical species concentrations conducted by different methods are compared. Physical and chemical consistency tests include: 1) sulfate (SO_4^{2-}) versus total sulfur (S), 2) soluble potassium (K^+) versus total potassium (K), 3) chloride (Cl^-) versus chlorine (Cl), and 4) ammonium balance.

3.3.2.1 Water-Soluble Sulfate (SO_4^{2-}) versus Total Sulfur (S)

SO_4^{2-} is measured by IC on quartz fiber filters and total S is measured by ED-XRF on Teflon filters. The theoretical ratio of SO_4^{2-} to S is approximately 3, based on their molecular weights and assuming all of the sulfur is present as SO_4^{2-}. Since SO_4^{2-} and total S are collected on different filters, this ratio is helpful for diagnosing flow rate problems of the samplers.

Figure 3 shows the scatter plots of SO_4^{2-} versus total S concentrations for each of the five sites. A good correlation ($R^2 = 0.99$) were observed for all the sites with a slope of 2.54±0.018 and an intercept of -0.059±0.051. The average sulfate to total sulfur ratio was determined to be 2.51±0.168, which meets the validation criteria (SO_4^{2-}/total S < 3.0).

Good correlations ($R^2 = 0.98–1.00$) were found for sulfate/total sulfur in $PM_{2.5}$ samples collected at individual sites. The regression statistics suggest a slope ranging from 2.51±0.041 to 2.60±0.037 and the intercepts are all at relatively low levels. The average sulfate/sulfur ratio ranges from 2.44±0.195 to 2.56±0.145 (Table 9). Both of the calculations indicate that the majority of the sulfur was present as soluble sulfate in $PM_{2.5}$.

Limits for outliers as suggested by USEPA [2012] are as follows,

Lower Limit: $[S]/[SO_4^{2-}] = 0.25$

Upper Limit: $[S]/[SO_4^{2-}] = 0.45$

11 samples are flagged as outliers and they were listed in Table 10 with the corresponding mass, SO_4^{2-}, S concentrations and the [S]/[SO_4^{2-}] ratios. Since the chemical information was obtained from two types of filter substrates, the % differences of masses obtained from Teflon filters and quartz fiber filters (column "T vs. Q %Diff") were also included for ease of reference. The main causes of the outliers may include: 1) larger sampling and measurement uncertainties due to the very low particle loading (3 samples, as highlighted in light blue, are with $PM_{2.5}$ mass concentrations below 10 $\mu g/m^3$) and 2) various sulfur existing in forms other than sulfate.

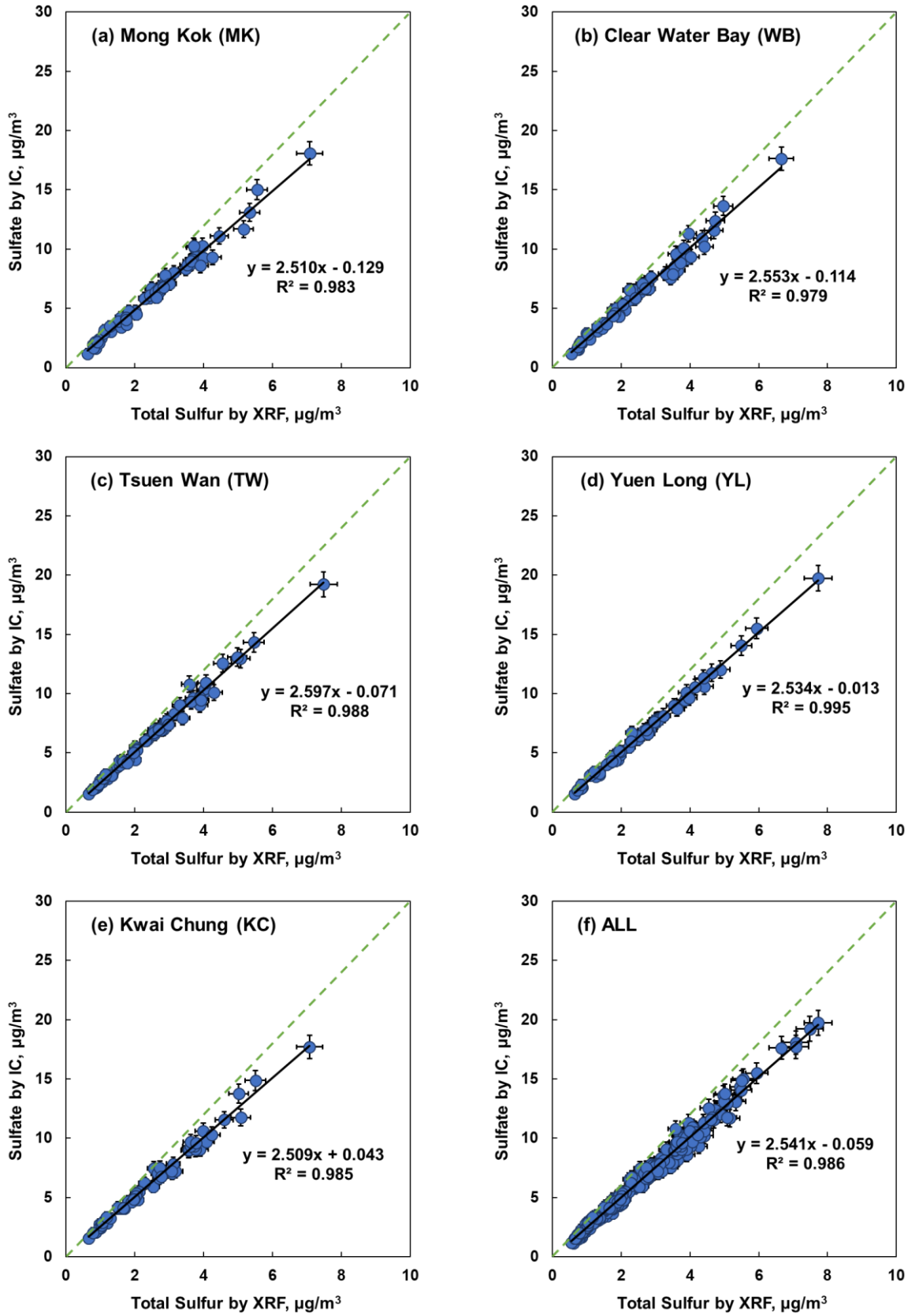

Figure 3. Scatter plots of sulfate versus total sulfur measurements for $PM_{2.5}$ samples collected at (a) MK, (b) WB, (c) TW, (d) YL, (e) KC, and (f) ALL.

Table 9. Statistics analysis of sulfate versus total sulfur measurements for $PM_{2.5}$ samples collected in this study (Quotation Ref. 16-02709).

Statistics/Site	MK	WB	TW	YL	KC	ALL
n	60	60	60	59	60	299
Slope	2.510 (±0.044)	2.553 (±0.049)	2.597 (±0.037)	2.534 (±0.024)	2.509 (±0.041)	2.541 (±0.018)
Intercept	-0.129 (±0.127)	-0.114 (±0.134)	-0.071 (±0.107)	-0.013 (±0.069)	0.043 (±0.118)	-0.059 (±0.051)
R^2	0.983	0.979	0.988	0.995	0.985	0.986
AVG total S	2.58	2.44	2.57	2.58	2.58	2.55
AVG SO_4^{2-}	6.36	6.12	6.60	6.52	6.51	6.42
AVG SO_4^{2-}/S	2.44 (±0.195)	2.49 (±0.194)	2.56 (±0.145)	2.53 (±0.124)	2.53 (±0.151)	2.51 (±0.168)

Table 10. List of flagged samples from the [S]/[SO_4^{2-}] test.

Sample ID	$PM_{2.5}$ mass conc. from Teflon Sample (µg/m^3)	$PM_{2.5}$ mass conc. from Quartz Sample (µg/m^3)	T vs. Q %Diff	SO_4^{2-} conc. (µg/m^3)	S conc. (µg/m^3)	[S]/[SO_4^{2-}] Ratio
MK170702	13.125	14.333	9%	1.632	0.858	0.526
MK170708	17.292	20.667	18%	2.091	0.959	0.459
MK170714	12.792	14.750	14%	1.170	0.620	0.529
MK170720	14.208	14.917	5%	1.661	0.804	0.484
MK170726	15.875	19.167	19%	3.424	1.599	0.467
MK171012	21.333	24.583	14%	3.642	1.752	0.481
MK171205	36.583	39.375	7%	9.313	4.256	0.457
WB170304	31.208	32.708	5%	7.560	3.438	0.455
WB170702	6.875	6.333	8%	1.524	0.757	0.497
WB170708	6.958	6.500	7%	1.547	0.715	0.462
WB170714	4.583	5.167	12%	1.179	0.549	0.466

3.3.2.2 Water-soluble Potassium (K^+) versus Total Potassium (K)

K^+ is measured by IC on quartz fiber filters and the total K is measured by ED-XRF on Teflon filters. The ratio of K^+ to K is expected to be equal to or less than 1. Figure 4 shows the scatter plots of K^+ versus total K concentrations for each of the five sites. A good correlation (R^2 = 0.96) were observed for all the sites with a slope of 0.81±0.010 and an intercept of -0.005±0.004. The ratio of water-soluble potassium to total potassium averages at 0.72±0.32, which meets the validation criteria (K^+/total K < 1).

Good correlations (R^2 = 0.94–0.97) were found for K^+/K in $PM_{2.5}$ samples collected at individual sites. The regression statistics suggested a slope ranging from 0.80±0.025 to 0.82±0.023 and the intercepts are all at relatively low levels (Table 11).

Generally, almost all of the total potassium is in its soluble ionic form.

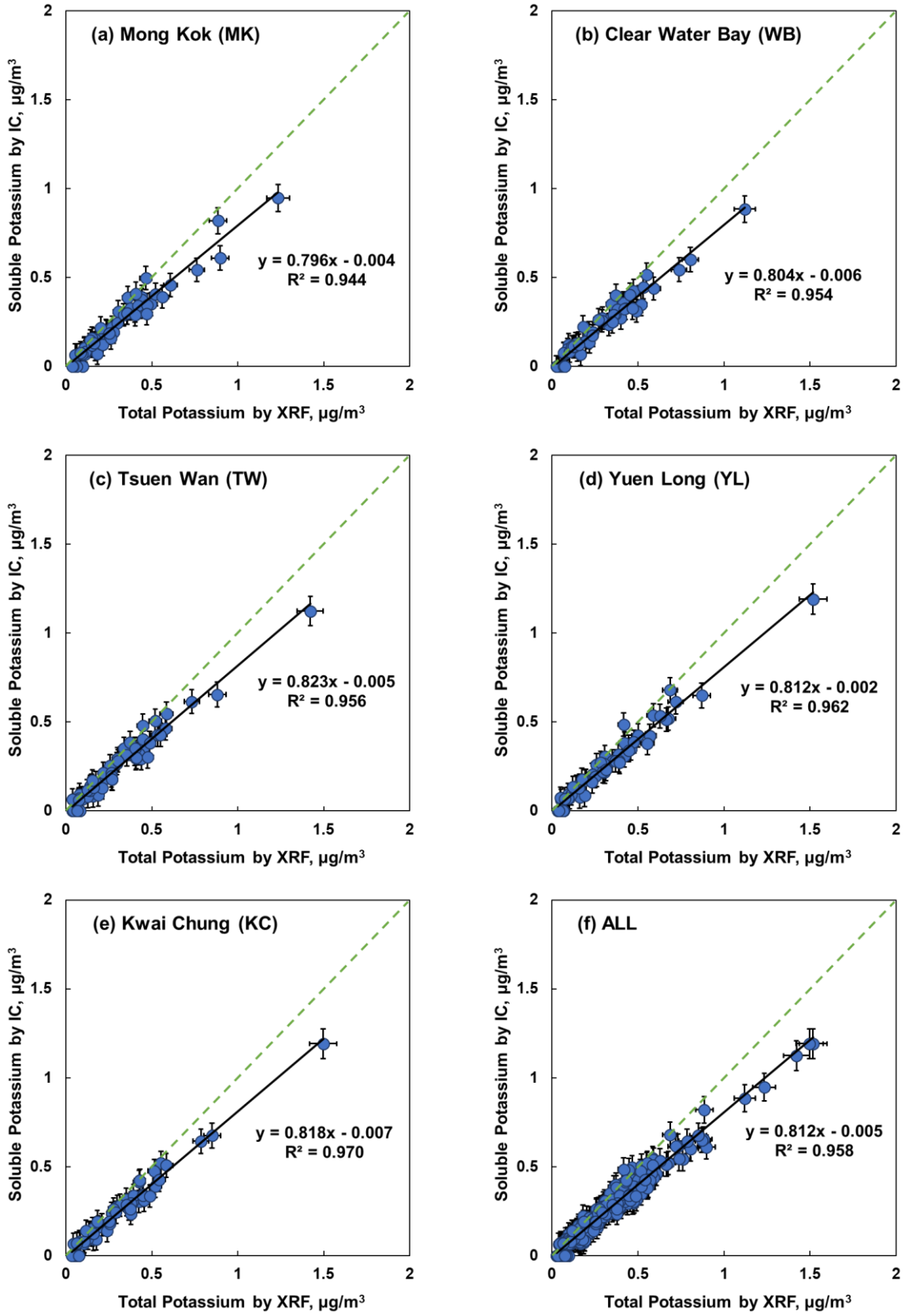

Figure 4. Scatter plots of water-soluble potassium versus total potassium measurements for $PM_{2.5}$ samples collected at (a) MK, (b) WB, (c) TW, (d) YL, (e) KC, and (f) ALL.

Table 11. Statistics analysis of water-soluble potassium versus total potassium measurements for $PM_{2.5}$ samples collected in this study (Quotation Ref. 16-02709).

Statistics/Site	MK	WB	TW	YL	KC	ALL
n	60	60	60	59	60	299
Slope	0.796 (±0.025)	0.804 (±0.023)	0.823 (±0.023)	0.812 (±0.021)	0.818 (±0.019)	0.812 (±0.010)
Intercept	-0.004 (±0.010)	-0.006 (±0.008)	-0.005 (±0.009)	-0.002 (±0.009)	-0.007 (±0.007)	-0.005 (±0.004)
R^2	0.944	0.954	0.956	0.962	0.970	0.958
AVG total K	0.301	0.267	0.291	0.323	0.293	0.295
AVG K^+	0.235	0.209	0.235	0.260	0.233	0.234
AVG K^+/K	0.720 (±0.301)	0.670 (±0.366)	0.738 (±0.339)	0.760 (±0.303)	0.734 (±0.309)	0.724 (±0.324)

3.3.2.3 Chloride (Cl^-) versus Chlorine (Cl)

Cl^- is measured by IC on quartz fiber filters and the total Cl is measured by ED-XRF on Teflon filters. The ratio of Cl^- to Cl is expected to equal or be less than 1. Figure 5 shows the scatter plots of Cl^- versus total Cl concentrations for each of the five sites. Moderate correlations (R^2 = 0.74) were found for the combined data of all the sampling sites. The slope deviates, to some degree, from unity (0.62–1.05). The uncertainties of Cl^-/Cl measurements are mainly associated with the volatility of Cl. On one hand, a portion of Cl^- could be lost during the storage of the quartz fiber filters especially when the aerosol samples are acidic. On the other hand, some Cl would be volatized in the vacuum chamber during the ED-XRF analysis. Such losses are more significant when Cl concentrations are low.

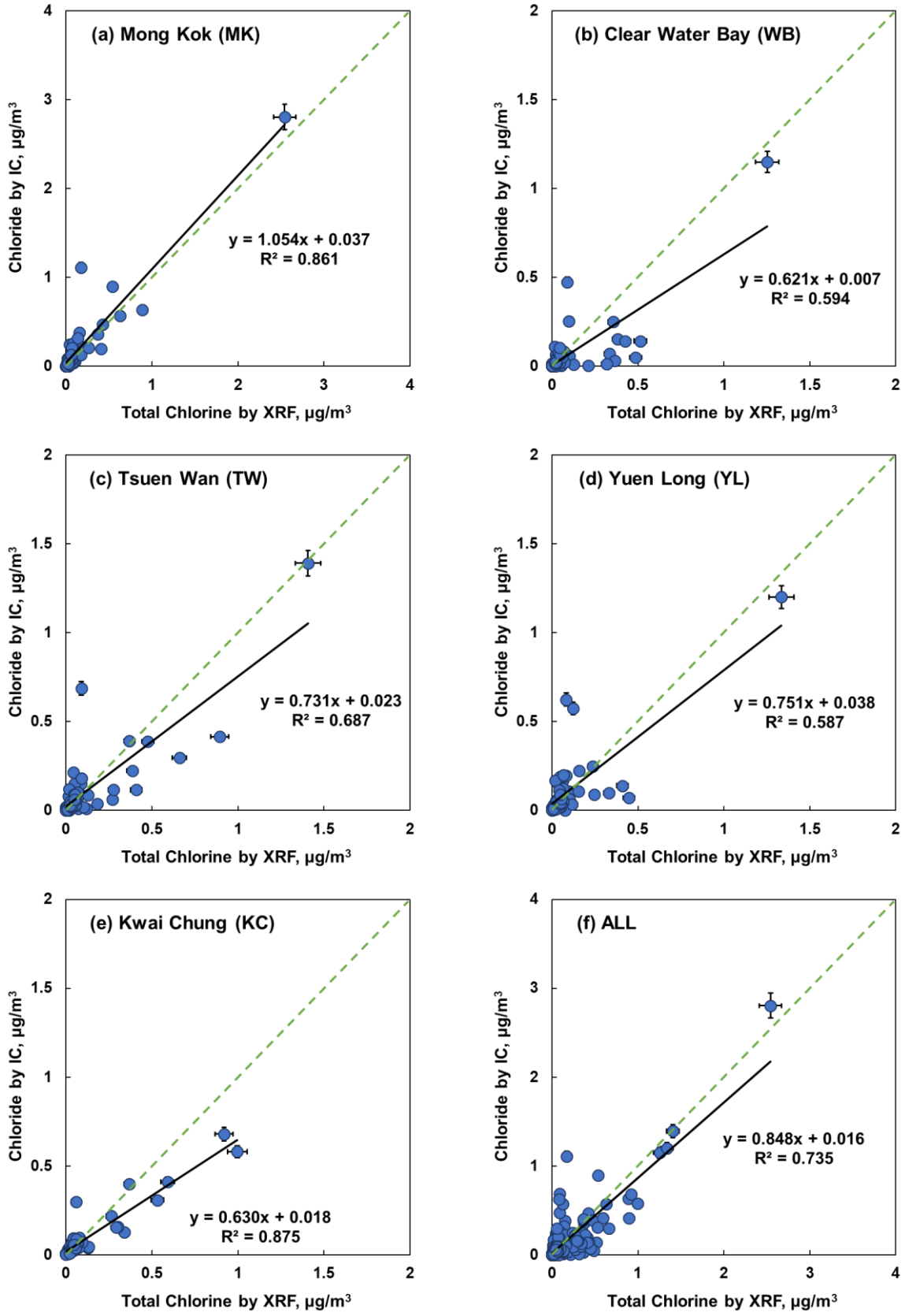

Figure 5. Scatter plots of chloride versus total chlorine measurements for $PM_{2.5}$ samples collected at (a) MK, (b) WB, (c) TW, (d) YL, (e) KC, and (f) ALL.

Table 12. Statistics analysis of chloride versus total chlorine measurements for $PM_{2.5}$ samples collected in this study (Quotation Ref. 16-02709).

Statistics/Site	MK	WB	TW	YL	KC	ALL
n	60	60	60	59	60	299
Slope	1.054 (±0.056)	0.621 (±0.067)	0.731 (±0.065)	0.751 (±0.083)	0.630 (±0.031)	0.848 (±0.030)
Intercept	0.037 (±0.021)	0.007 (±0.015)	0.023 (±0.017)	0.038 (±0.017)	0.018 (±0.007)	0.016 (±0.008)
R^2	0.861	0.594	0.687	0.587	0.875	0.735
AVG total Cl	0.147	0.105	0.123	0.092	0.109	0.115
AVG Cl^-	0.191	0.072	0.113	0.107	0.087	0.114
AVG Cl^-/Cl	1.65 (±1.27)	1.20 (±1.29)	1.43 (±1.59)	1.76 (±1.76)	1.10 (±0.79)	1.43 (±1.39)

3.3.2.4 Ammonium Balance

To further validate the ion measurements, calculated versus measured ammonium (NH_4^+) are compared. NH_4^+ is directly measured by IC analysis of quartz fiber filter extract. NH_4^+ is very often found in the chemical forms of NH_4NO_3, $(NH_4)_2SO_4$, and NH_4HSO_4 while NH_4Cl is usually negligible and excluded from the calculation. Assuming full neutralization, measured NH_4^+ can be compared with the computed NH_4^+, which can be calculated in the following two ways,

Calculated NH_4^+ based on NH_4NO_3 and $(NH_4)_2SO_4 = 0.29 \times [NO_3^-] + 0.374 \times [SO_4^{2-}]$

Calculated NH_4^+ based on NH_4NO_3 and $NH_4HSO_4 = 0.29 \times [NO_3^-] + 0.187 \times [SO_4^{2-}]$

The calculated NH_4^+ is plotted against measured NH_4^+ for each of the five sites in Figure 6. For both forms of sulfate the comparisons show strong correlations ($R^2 = 0.97$) but with quite different slopes. The slopes for individual sampling sites range from 0.98±0.023 at MK to 1.02±0.029 at WB assuming ammonium sulfate, and from 0.55±0.014 at WB to 0.59±0.013 at YL assuming ammonium bisulfate. These values were close to those found in earlier years. The average ratios of calculated ammonium to measured ammonium (see Table 13) suggest that ammonium sulfate is the dominant form for sulfate in the $PM_{2.5}$ over the Hong Kong region in the year of 2017.

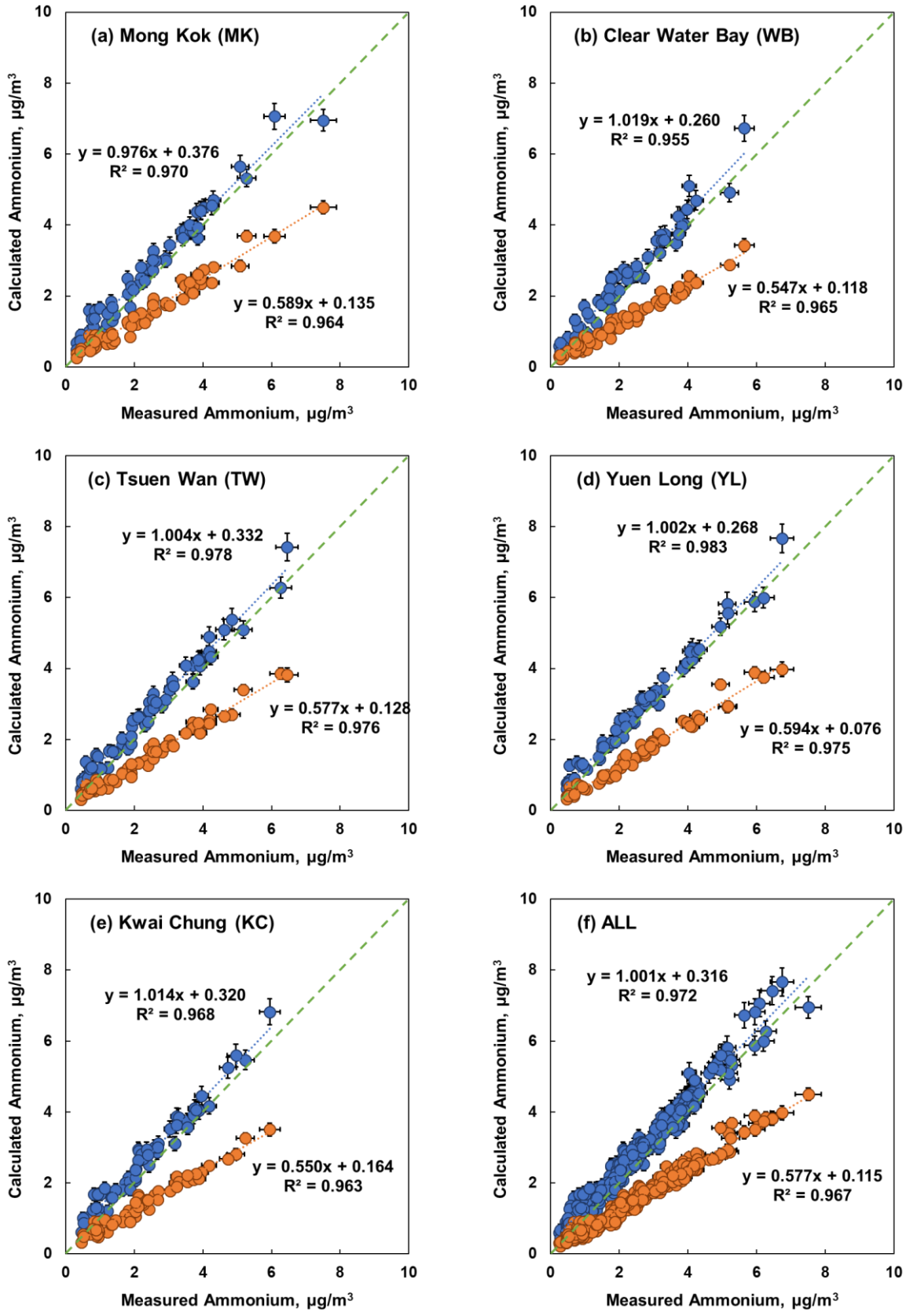

Figure 6. Scatter plots of calculated ammonium versus measured ammonium for $PM_{2.5}$ samples collected at (a) MK, (b) WB, (c) TW, (d) YL, (e) KC, and (f) ALL. The calculated ammonium data are obtained assuming all nitrate was in the form of ammonium nitrate and all sulfate was in the form of either ammonium sulfate (data in blue) or ammonium bisulfate (data in orange).

Table 13. Statistics analysis of calculated ammonium versus measured ammonium for $PM_{2.5}$ samples collected in this study (Quotation Ref. 16-02709).

Statistics/Site	MK	WB	TW	YL	KC	ALL
n	60	60	60	59	60	299
Ammonium Sulfate (blue dots)						
Slope	0.976 (±0.023)	1.019 (±0.029)	1.004 (±0.020)	1.002 (±0.018)	1.014 (±0.024)	1.001 (±0.010)
Intercept	0.376 (±0.065)	0.260 (±0.071)	0.332 (±0.056)	0.268 (±0.052)	0.320 (±0.064)	0.316 (±0.027)
R^2	0.970	0.955	0.978	0.983	0.968	0.972
AVG Mea. NH_4^+	2.45	2.12	2.41	2.52	2.29	2.36
AVG Cal. NH_4^+	2.77	2.42	2.76	2.79	2.64	2.68
AVG Cal./Mea. NH_4^+	1.24 (±0.305)	1.24 (±0.309)	1.24 (±0.260)	1.19 (±0.232)	1.23 (±0.242)	1.23 (±0.270)
Ammonium Bisulfate (orange dots)						
Slope	0.589 (±0.015)	0.547 (±0.014)	0.577 (±0.012)	0.594 (±0.013)	0.550 (±0.014)	0.577 (±0.006)
Intercept	0.135 (±0.043)	0.118 (±0.034)	0.128 (±0.033)	0.076 (±0.037)	0.164 (±0.037)	0.115 (±0.017)
R^2	0.964	0.965	0.976	0.975	0.963	0.967
AVG Mea. NH_4^+	2.45	2.12	2.41	2.52	2.29	2.36
AVG Cal. NH_4^+	1.58	1.28	1.52	1.57	1.42	1.47
AVG Cal./Mea. NH_4^+	0.70 (±0.170)	0.65 (±0.157)	0.67 (±0.136)	0.65 (±0.119)	0.66 (±0.136)	0.67 (±0.145)

3.3.3 Charge Balance

For the anion and cation balance, the sum of Cl^-, NO_3^-, and SO_4^{2-} is compared to the sum of NH_4^+, Na^+, and K^+ in μeq/m^3 using the following equations:

$$\mu eq/m^3 \text{ for anions } = \left(\frac{Cl^-}{35.453} + \frac{NO_3^-}{62.005} + \frac{SO_4^{2-}}{96/2} \right)$$

$$\mu eq/m^3 \text{ for cations } = \left(\frac{NH_4^+}{18.04} + \frac{Na^+}{23.0} + \frac{K^+}{39.098} \right)$$

The anion equivalents are plotted against the cation equivalents in Figure 7. A strong correlation ($R^2 = 0.99$) was observed for the $PM_{2.5}$ samples collected at all of the sampling sites. Seen from Figure 7, the slopes obtained from individual sites range from 0.98±0.013 to 1.00±0.018 while the average Σanion/Σcation ratios range from 0.98±0.075 to 1.01±0.062 (Table 14).

The limits used for identifying outliers suggested by USEPA [2012] are as follows,

Lower Limit: [Sum of Anions]/[Sum of Cations] = 0.86

Upper Limit: [Sum of Anions]/[Sum of Cations] = 2.82

Based on these criteria, 4 samples were identified as outliers in this dataset and they are listed in Table 15 with the corresponding mass concentrations and the Σanion/Σcation ratios.

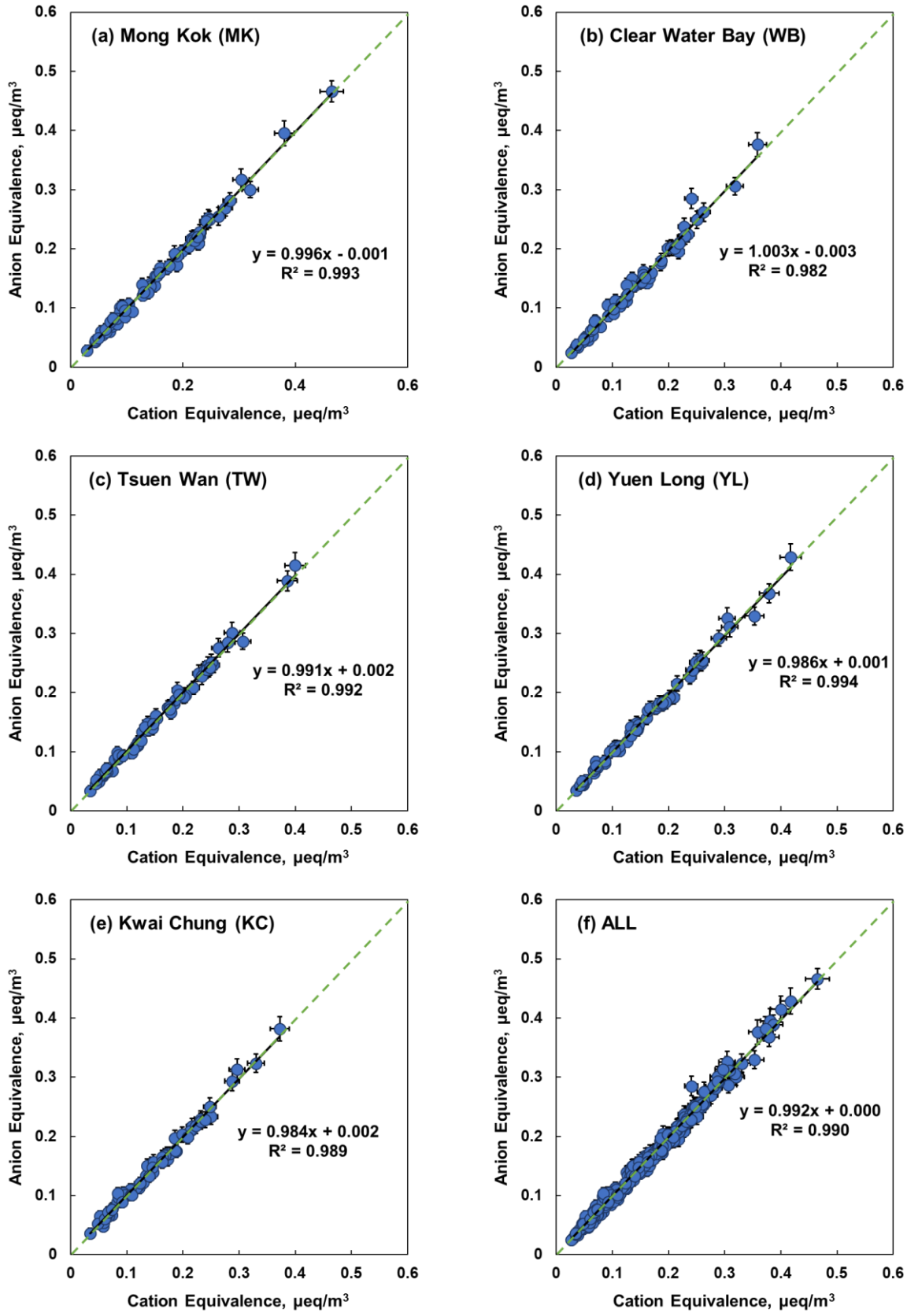

Figure 7. Scatter plots of anion versus cation measurements for $PM_{2.5}$ samples collected at (a) MK, (b) WB, (c) TW, (d) YL, (e) KC, and (f) ALL.

Table 14. Statistics analysis of anion versus cation measurements for $PM_{2.5}$ samples collected in this study (Quotation Ref. 16-02709).

Statistics/Site	MK	WB	TW	YL	KC	ALL
n	60	60	60	59	60	299
Slope	0.996 (±0.011)	1.003 (±0.018)	0.991 (±0.011)	0.986 (±0.010)	0.984 (±0.013)	0.992 (±0.006)
Intercept	-0.001 (±0.002)	-0.003 (±0.003)	0.002 (±0.002)	0.001 (±0.002)	0.002 (±0.002)	0.000 (±0.001)
R^2	0.993	0.982	0.992	0.994	0.989	0.990
AVG ∑cation	0.161	0.139	0.156	0.160	0.150	0.153
AVG ∑anion	0.160	0.137	0.157	0.158	0.149	0.152
AVG ∑anion/∑cation	0.992 (±0.061)	0.979 (±0.075)	1.014 (±0.062)	0.994 (±0.048)	1.005 (±0.072)	0.997 (±0.065)

Table 15. List of flagged samples from the charge balance test.

Sample ID	$PM_{2.5}$ mass conc. from Teflon Sample ($\mu g/m^3$)	$PM_{2.5}$ mass conc. from Quartz Sample ($\mu g/m^3$)	∑anion eqv., ($\mu eq/m^3$)	∑cation eqv., ($\mu eq/m^3$)	∑anion/∑cation Ratio
MK171018	18.292	21.042	0.094	0.110	0.854
WB170226	7.667	8.833	0.046	0.057	0.809
WB170515	6.958	8.750	0.054	0.064	0.837
KC170226	8.792	9.875	0.048	0.058	0.837

3.3.4 TOT versus TOR for Carbon Measurements

Carbon concentrations were determined for the collected $PM_{2.5}$ samples by both TOR and TOT methods. The comparison results of OC and EC determined by both methods for individual sites are shown in Figure 8. Generally, EC concentrations derived by the TOT method were much lower than those by the TOR method. The difference in EC obtained by these two methods has been well-documented and is primarily a result of method-dependent nature of correction of charring of OC formed during thermal analysis [e.g., Chow et al.,2004; Chen et al., 2004]. Seen from the results, the average ratios of TOT EC to TOR EC for samples from individual sampling sites range from 0.72±0.11 at YL to 0.76±0.10 at TW (Table 16).

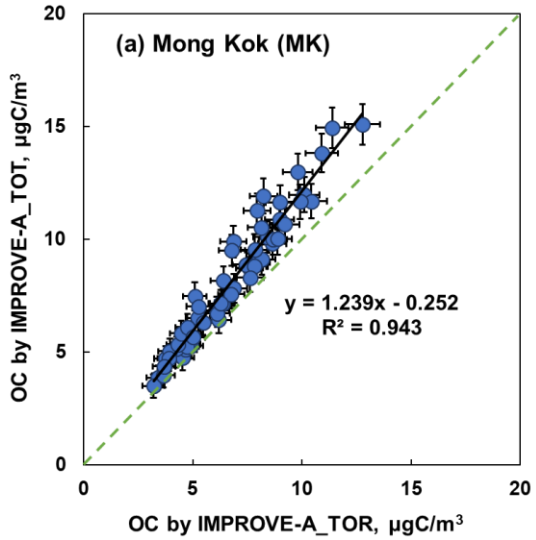
(a) Mong Kok (MK)
y = 1.239x - 0.252
R² = 0.943
OC by IMPROVE-A_TOR, µgC/m³
OC by IMPROVE-A_TOT, µgC/m³

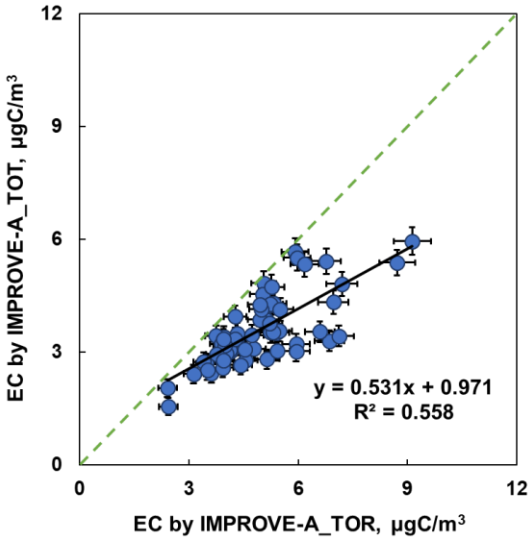
y = 0.531x + 0.971
R² = 0.558
EC by IMPROVE-A_TOR, µgC/m³
EC by IMPROVE-A_TOT, µgC/m³

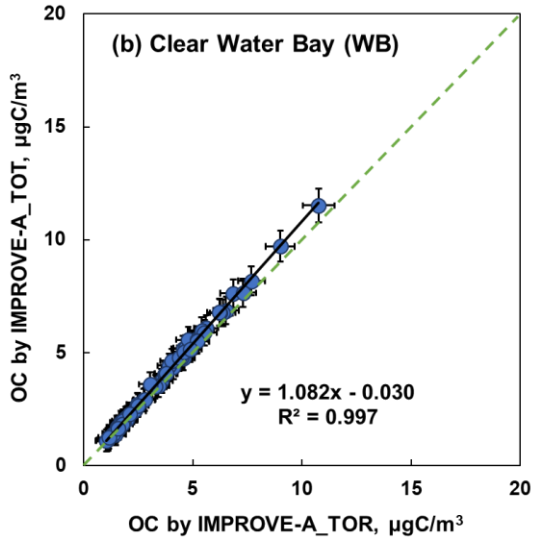
(b) Clear Water Bay (WB)
y = 1.082x - 0.030
R² = 0.997
OC by IMPROVE-A_TOR, µgC/m³
OC by IMPROVE-A_TOT, µgC/m³

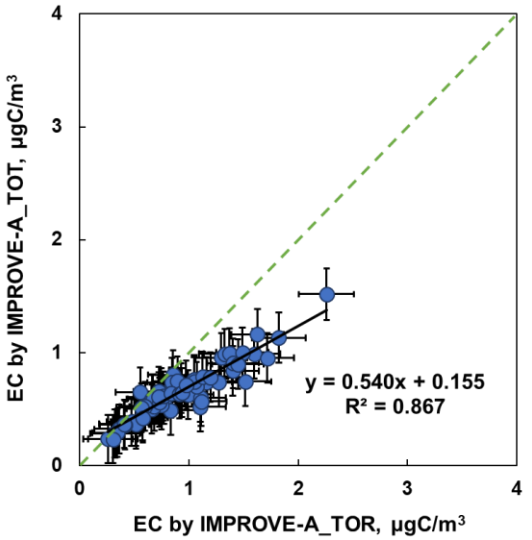
y = 0.540x + 0.155
R² = 0.867
EC by IMPROVE-A_TOR, µgC/m³
EC by IMPROVE-A_TOT, µgC/m³

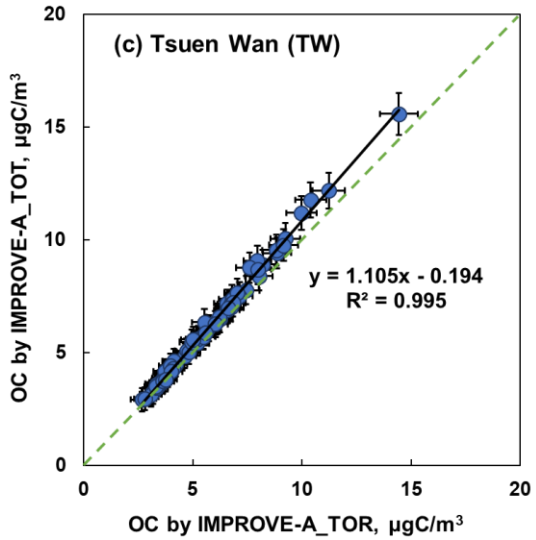
(c) Tsuen Wan (TW)
y = 1.105x - 0.194
R² = 0.995
OC by IMPROVE-A_TOR, µgC/m³
OC by IMPROVE-A_TOT, µgC/m³

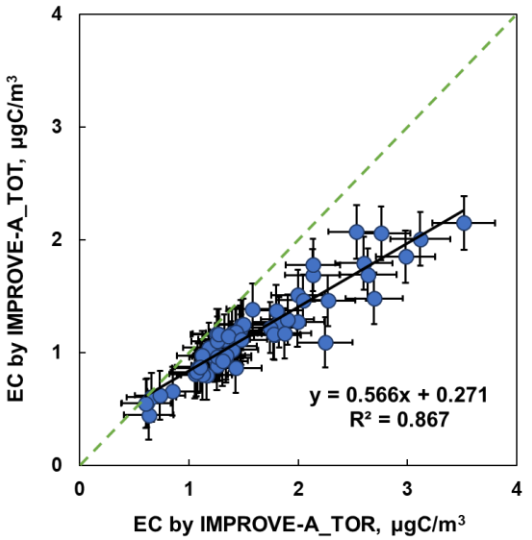
y = 0.566x + 0.271
R² = 0.867
EC by IMPROVE-A_TOR, µgC/m³
EC by IMPROVE-A_TOT, µgC/m³

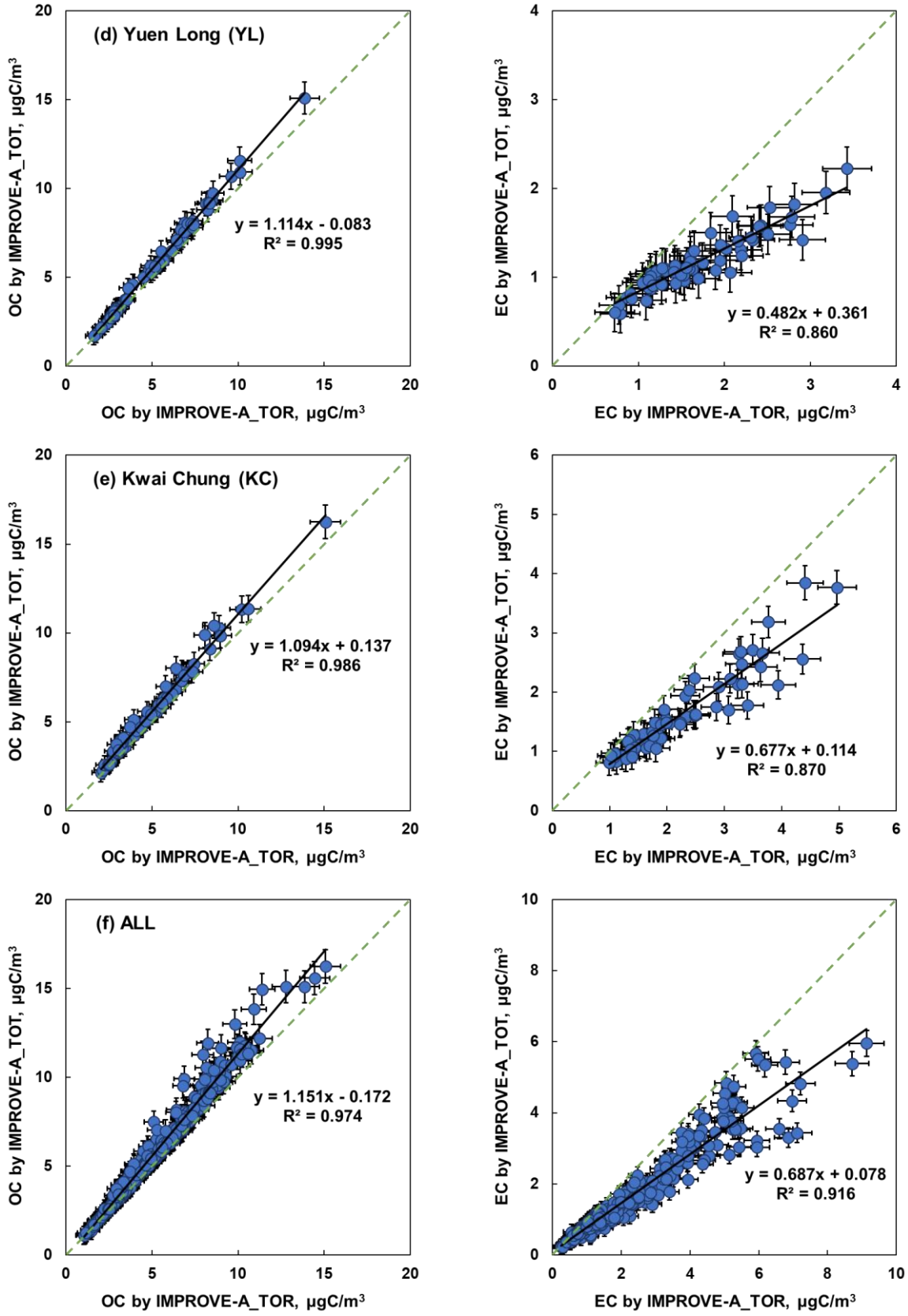

Figure 8. Comparisons of OC and EC determined by TOR and TOT methods for $PM_{2.5}$ samples collected at (a) MK, (b) WB, (c) TW, (d) YL, (e) KC, and (f) ALL.

Table 16. Statistics analysis of OC and EC determined by TOR and TOT methods for $PM_{2.5}$ samples collected in this study (Quotation Ref. 16-02709).

Statistics/Site	MK	WB	TW	YL	KC	ALL
n	60	60	60	59	60	299
TOT OC versus TOR OC						
Slope	1.239 (±0.040)	1.082 (±0.008)	1.105 (±0.011)	1.114 (±0.010)	1.094 (±0.017)	1.151 (±0.011)
Intercept	-0.252 (±0.284)	-0.030 (±0.033)	-0.194 (±0.067)	-0.083 (±0.059)	0.137 (±0.098)	-0.172 (±0.064)
R^2	0.943	0.997	0.995	0.995	0.986	0.974
AVG TOR_OC	6.72	3.73	5.90	5.29	5.14	5.36
AVG TOT_OC	8.07	4.01	6.33	5.81	5.76	6.00
AVG TOT_OC/TOR_OC	1.20 (±0.101)	1.07 (±0.038)	1.07 (±0.033)	1.09 (±0.041)	1.12 (±0.068)	1.11 (±0.078)
TOT EC versus TOR EC						
Slope	0.531 (±0.062)	0.540 (±0.028)	0.566 (±0.029)	0.482 (±0.026)	0.677 (±0.034)	0.687 (±0.012)
Intercept	0.971 (±0.317)	0.155 (±0.028)	0.271 (±0.050)	0.361 (±0.047)	0.114 (±0.085)	0.078 (±0.034)
R^2	0.558	0.867	0.867	0.860	0.870	0.916
AVG TOR_EC	4.95	0.93	1.60	1.70	2.28	2.29
AVG TOT_EC	3.59	0.66	1.18	1.18	1.66	1.65
AVG TOT_EC/TOR_EC	0.738 (±0.120)	0.742 (±0.128)	0.758 (±0.100)	0.724 (±0.111)	0.739 (±0.098)	0.740 (±0.112)

3.3.5 Material Balance

Major PM components can be classified into the following categories: 1) geological material, which can be estimated by (1.89 × [Al] + 2.14 × [Si] + 1.4 × [Ca] + 1.43 × [Fe]); 2) organic matter, which can be estimated from OC concentration as [OM] = 1.4 × [OC]; 3) soot which can be represented by EC concentration; 4) ammonium; 5) sulfate; 6) nitrate; 7) non-crustal trace elements; and 8) unidentified material. Considering the large uncertainty in Na measurement by ED-XRF, water-soluble sodium is used in calculation instead of total sodium. Therefore, the reconstructed mass is calculated by the following equation,

[Reconstructed Mass]

= $1.89 \times [Al] + 2.14 \times [Si] + 1.4 \times [Ca] + 1.43 \times [Fe]$

+ $1.4 \times [OC]$

+ [EC]

+ $[NH_4^+]$

+ $[Na^+]$

+ [K]

+ $[SO_4^{2-}]$

+ $[NO_3^-]$

+ trace elements excluding Na, Al, Si, K, Ca, Fe, and S

The reconstructed mass is plotting against the measured mass in Figure 9. A strong correlation ($R^2 = 0.98$) is observed between the reconstructed mass and measured mass with a slope of 0.88±0.007. Different from the comparison made between sum of chemical species and measured mass (Figure 2), the major uncertainty of the reconstructed mass is due to the estimation of organic matter (OM). Generally, the concentration of OM is determined by multiplying the OC concentration by an empirical factor. It is worth noting that the [OM]/[OC] ratio is site dependent. The [OM]/[OC] ratio of freshly emitted aerosols is usually smaller than that of the more aging (oxygenated) aerosols. In this study where a value of 1.4 was applied to this factor, it can be seen from Table 17 that the reconstructed masses at all the sites agree very well with the measured masses.

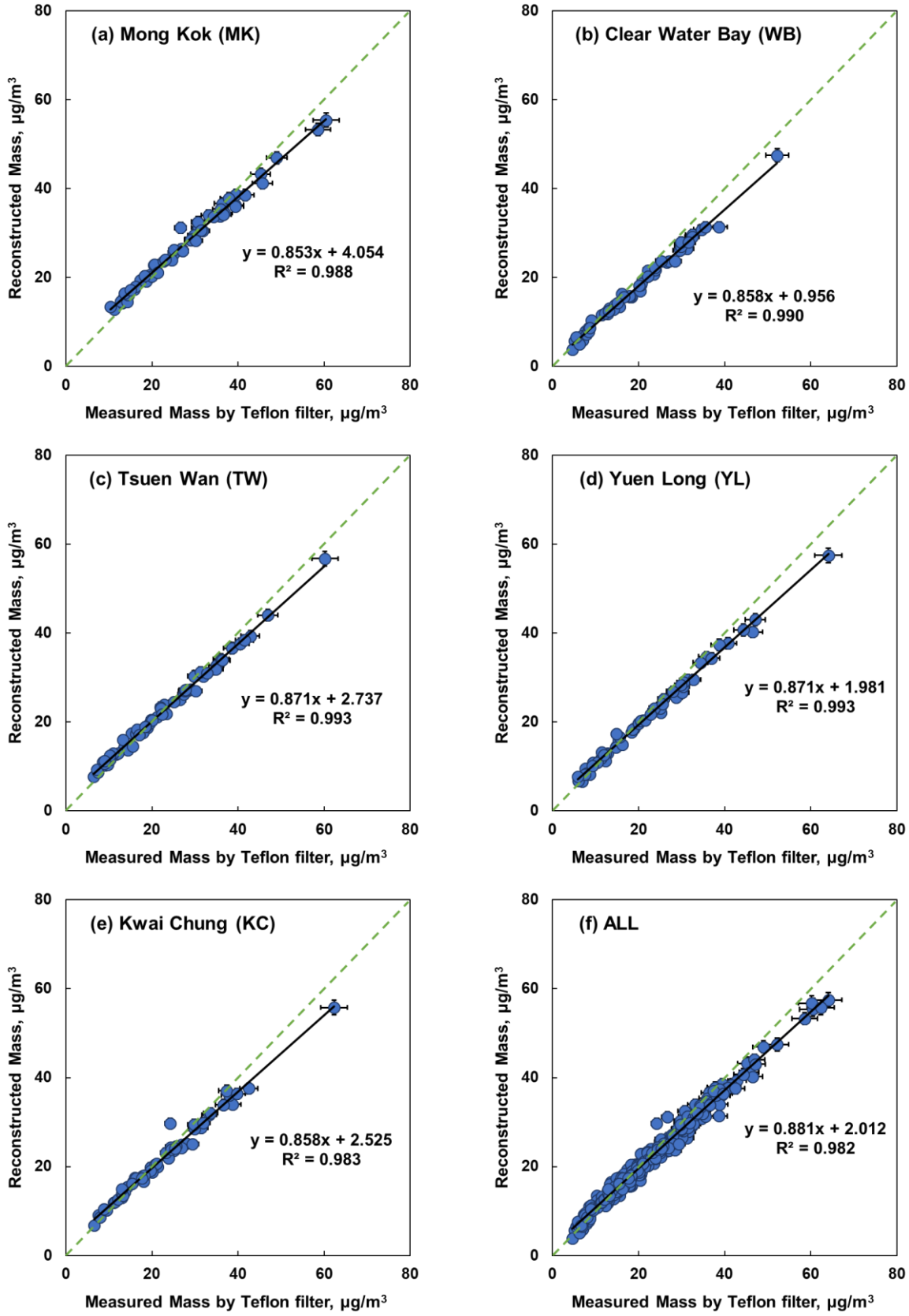

Figure 9. Scatter plots of reconstructed mass versus measured mass on Teflon filters for $PM_{2.5}$ samples collected at (a) MK, (b) WB, (c) TW, (d) YL, (e) KC, and (f) ALL.

Table 17. Statistics analysis of reconstructed mass versus measured mass on Teflon filters for $PM_{2.5}$ samples collected in this study (Quotation Ref. 16-02709).

Statistics/Site	MK	WB	TW	YL	KC	ALL
n	60	60	60	59	60	299
Slope	0.853 (±0.012)	0.858 (±0.011)	0.871 (±0.009)	0.871 (±0.009)	0.858 (±0.015)	0.881 (±0.007)
Intercept	4.054 (±0.364)	0.956 (±0.235)	2.737 (±0.238)	1.981 (±0.240)	2.525 (±0.364)	2.012 (±0.173)
R^2	0.988	0.990	0.993	0.993	0.983	0.982
AVG Mea. Mass	27.18	18.67	22.38	22.50	22.08	22.56
AVG Rec. Mass	27.24	16.98	22.23	21.58	21.46	21.90
AVG Rec./Mea. Mass	1.03 (±0.084)	0.93 (±0.074)	1.03 (±0.101)	0.99 (±0.089)	1.00 (±0.083)	1.00 (±0.094)

The annual average composition (%) of the major components to the $PM_{2.5}$ mass is shown in Figure 10 for individual sites. Overall, the reconstructed mass agrees very well with the measured mass using an [OM]-to-[OC] ratio of 1.4.

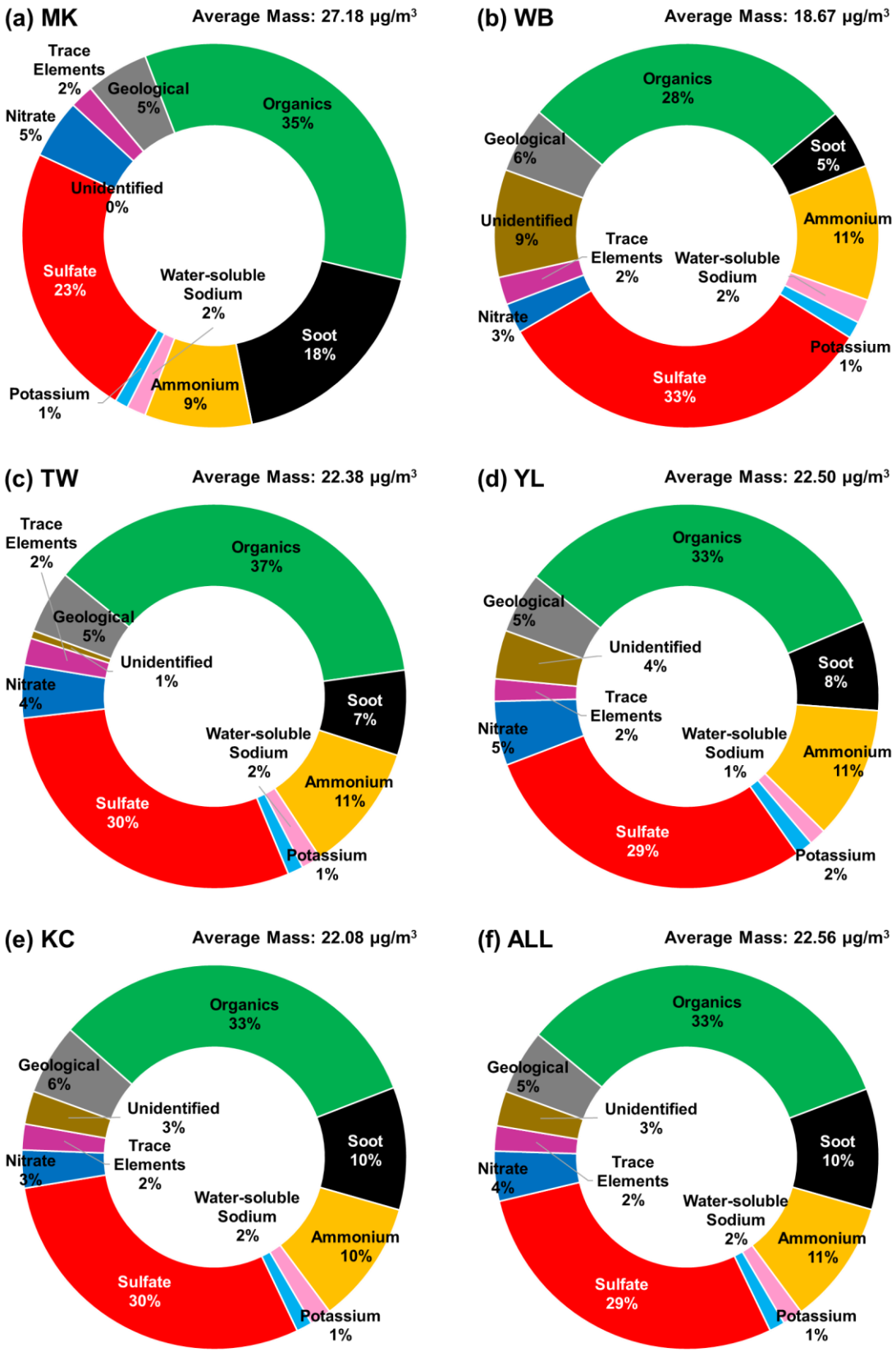

Figure 10. Annual average composition (%) of major components including 1) geological material; 2) organic matter; 3) soot; 4) ammonium; 5) sulfate; 6) nitrate; 7) non-crustal trace elements, and 8) Unidentified material (difference between measured mass and the reconstructed mass) to $PM_{2.5}$ mass for (a) MK, (b) WB, (c) TW, (d) YL, (e) KC, and (f) ALL.

Annually MK had the highest $PM_{2.5}$ loading while WB had the lowest (Figure 11). For all of the five sites, sulfate and OM were the two most abundant components followed by ammonium and soot (EC by TOR method). The EC concentration was the highest at MK and the lowest at WB, which is consistent with their respective site characteristics. The concentrations of sulfate, ammonium, geological materials, and trace elements did not vary much across all five sites.

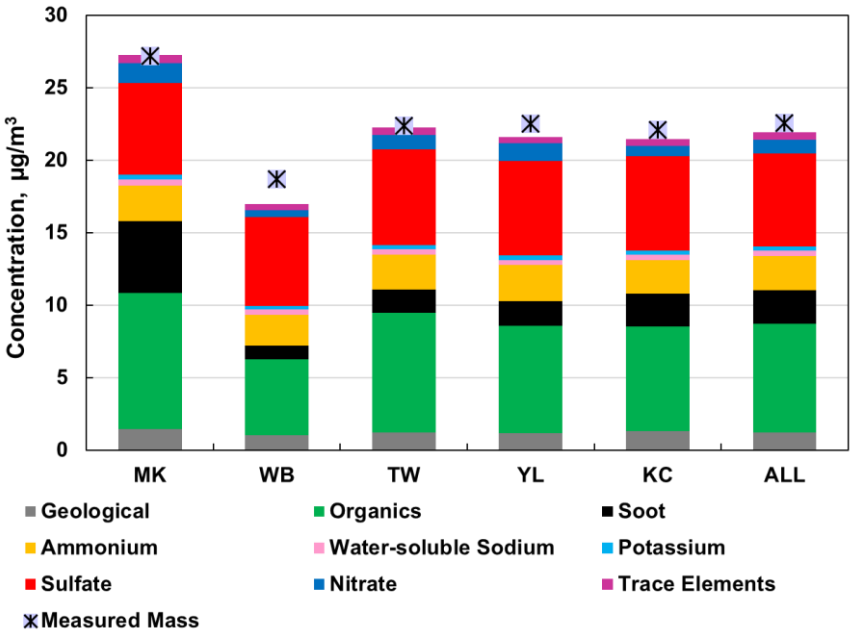

Figure 11. Comparison of annual average concentrations of major components including 1) geological material; 2) organic matter; 3) soot; 4) ammonium; 5) water-soluble sodium; 6) potassium; 7) sulfate; 8) nitrate, and 9) non-crustal trace elements and the $PM_{2.5}$ mass between individual sites.

3.3.6 Analysis of Collocated Data

In the Hong Kong $PM_{2.5}$ speciation network, two sites were equipped with collocated samplers during 2017, as shown in Table 2. The MK site included a third Partisol sampler for Teflon filters while the WB site included a third Partisol sampler for quartz fiber filters. The collocated samplers were operated on a 1-in-6 day schedule as the primary samplers did.

Figures 12–19 show examples of the comparisons for $PM_{2.5}$ mass concentration by gravimetric analysis, potassium, calcium, and iron by ED-XRF, ammonium and sulfate by IC, OC and EC by the TOR method, respectively. The least-squares linear regression parameters (slope, intercept, and R^2) by sites for each of these species are also included in the tables placed right below the respective figures (Tables 18–25). These figures demonstrate from good to excellent agreement for the major analytes.

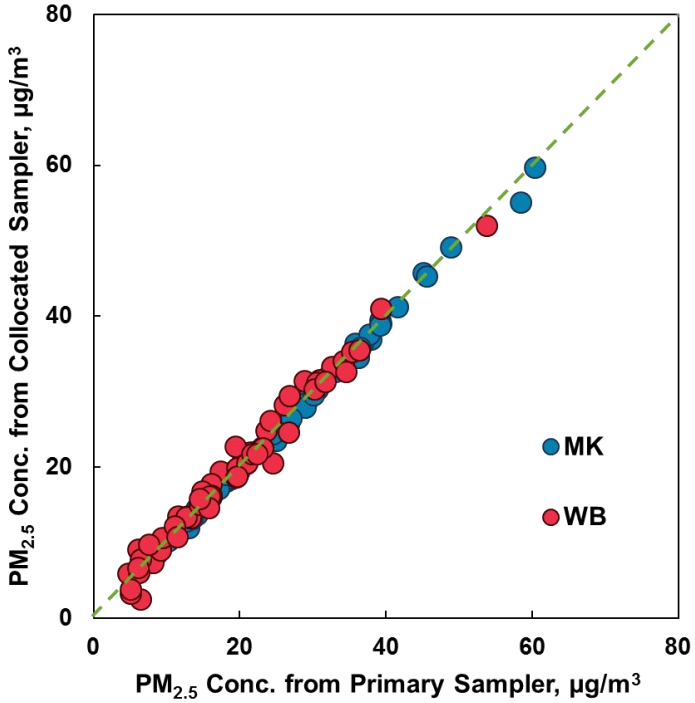

Figure 12. Collocated data for $PM_{2.5}$ concentrations at MK and WB sites during 2017.

Table 18. Statistics analysis of collocated data for $PM_{2.5}$ concentrations at MK and WB sites during 2017.

Statistics/Site	MK	WB
n	60	60
Slope	0.980 (±0.007)	0.986 (±0.018)
Intercept	0.081 (±0.197)	0.391 (±0.402)
R^2	0.997	0.980

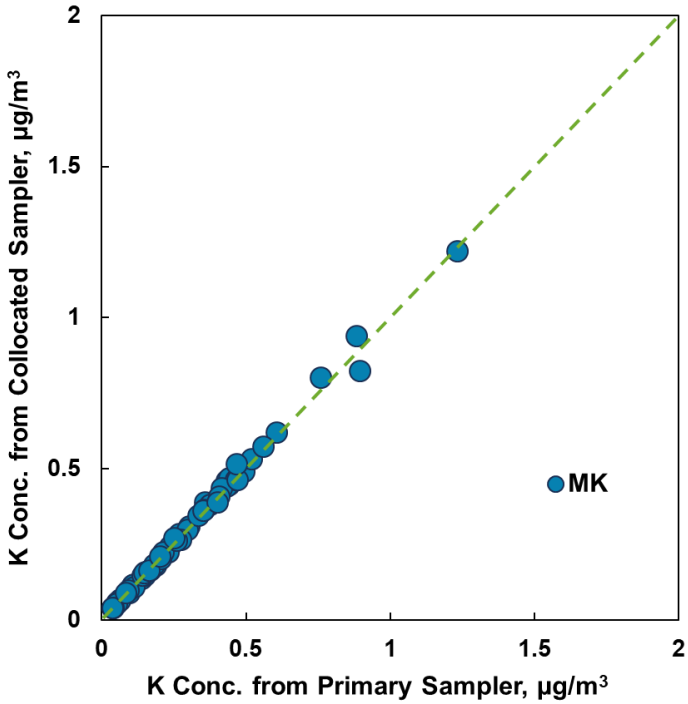

Figure 13. Collocated data for potassium concentrations at MK site during 2017.

Table 19. Statistics analysis of collocated data for potassium concentrations at MK site during 2017.

Statistics/Site	MK
n	60
Slope	1.00 (±0.009)
Intercept	0.001 (±0.004)
R^2	0.995

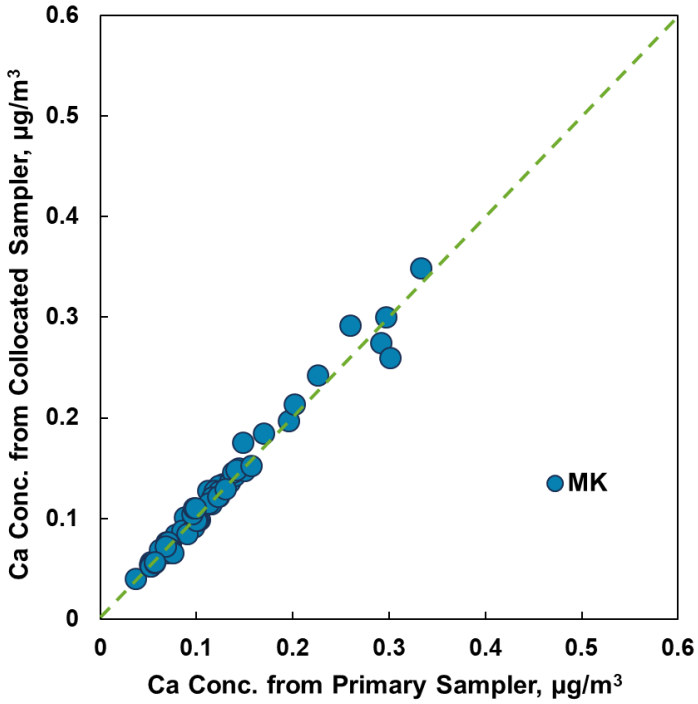

Figure 14. Collocated data for calcium concentrations at MK site during 2017.

Table 20. Statistics analysis of collocated data for calcium concentrations at MK site during 2017.

Statistics/Site	MK
n	60
Slope	0.999 (±0.020)
Intercept	0.002 (±0.003)
R^2	0.978

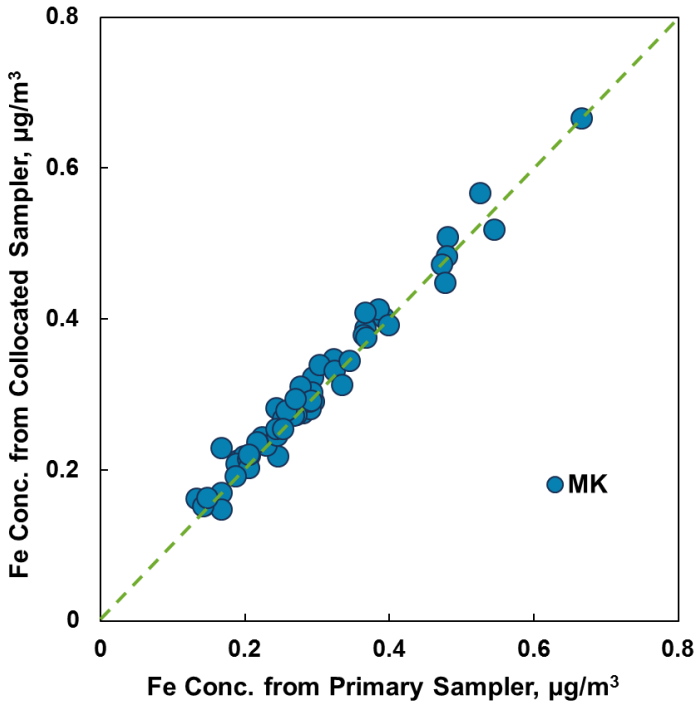

Figure 15. Collocated data for iron concentrations at MK site during 2017.

Table 21. Statistics analysis of collocated data for iron concentrations at MK site during 2017.

Statistics/Site	MK
n	60
Slope	0.973 (±0.020)
Intercept	0.017 (±0.006)
R^2	0.975

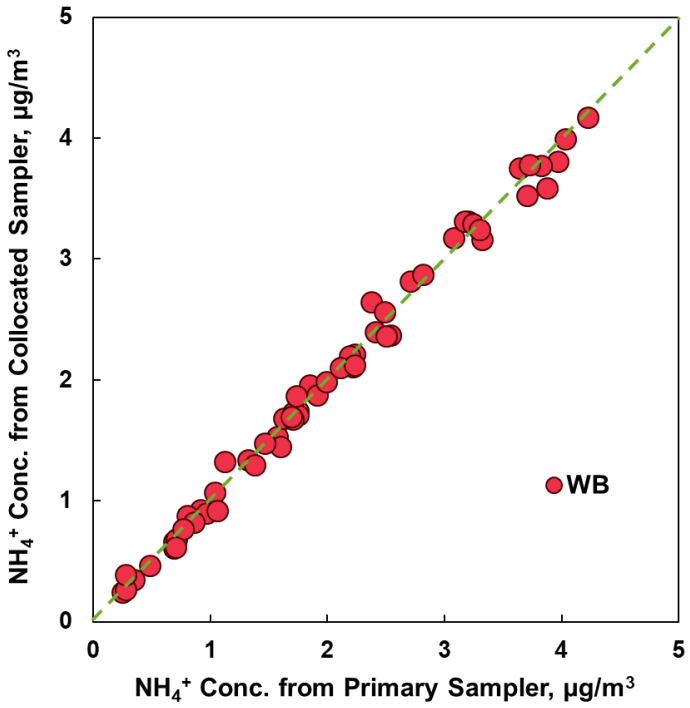

Figure 16. Collocated data for ammonium concentrations at WB site during 2017.

Table 22. Statistics analysis of collocated data for ammonium concentrations at WB site during 2017.

Statistics/Site	WB
n	60
Slope	0.994 (±0.011)
Intercept	-0.009 (±0.028)
R^2	0.993

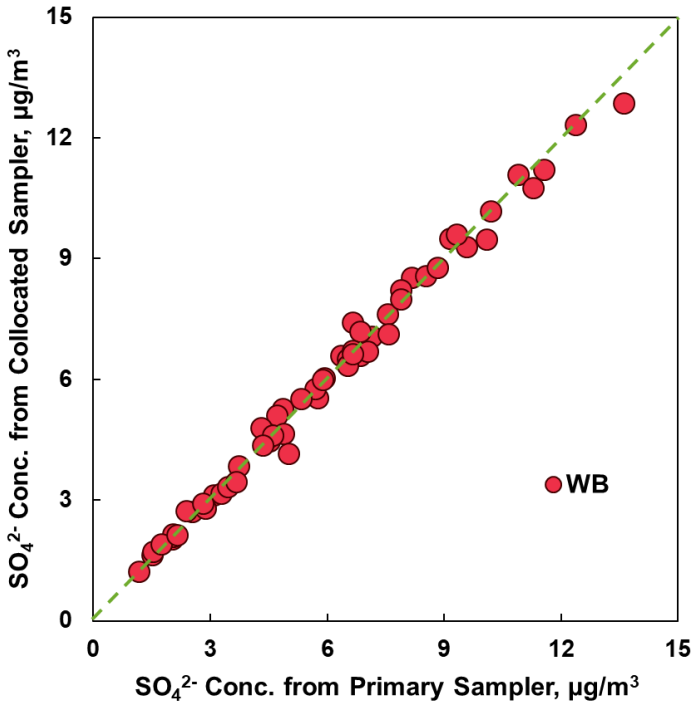

Figure 17. Collocated data for sulfate concentrations at WB site during 2017.

Table 23. Statistics analysis of collocated data for sulfate concentrations at WB site during 2017.

Statistics/Site	WB
n	60
Slope	0.964 (±0.011)
Intercept	0.185 (±0.076)
R^2	0.993

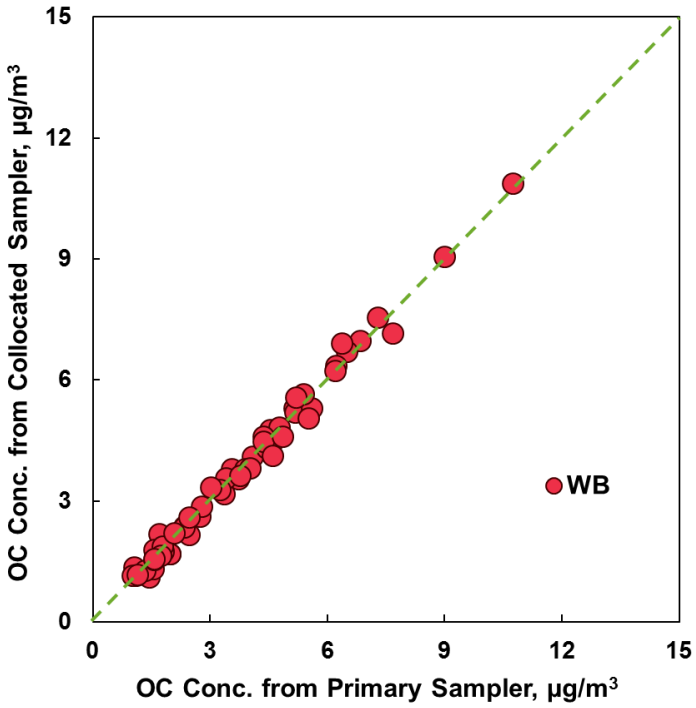

Figure 18. Collocated data for TOR OC concentrations at WB site during 2017.

Table 24. Statistics analysis of collocated data for TOR OC concentrations at WB site during 2017.

Statistics/Site	WB
n	60
Slope	1.01 (±0.014)
Intercept	-0.057 (±0.060)
R^2	0.989

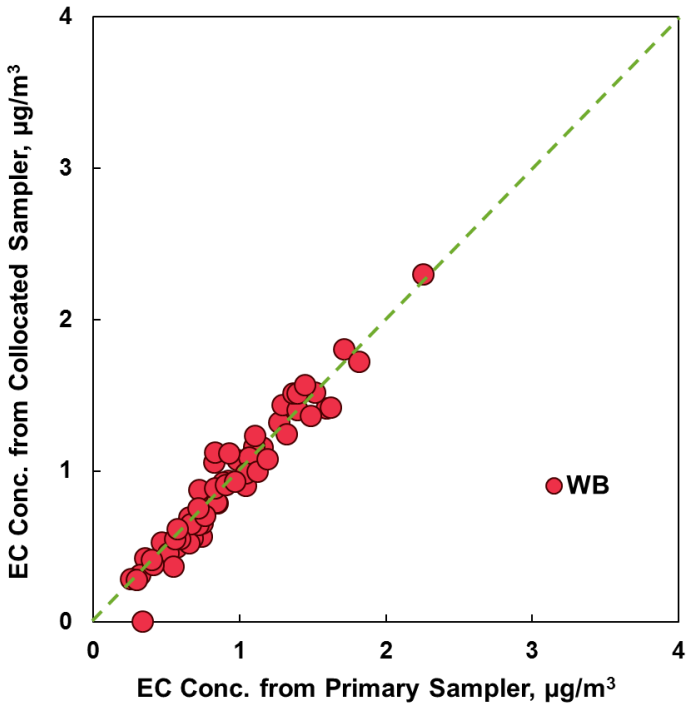

Figure 19. Collocated data for TOR EC concentrations at WB site during 2017.

Table 25. Statistics analysis of collocated data for TOR EC concentrations at WB site during 2017.

Statistics/Site	WB
n	58
Slope	1.02 (±0.034)
Intercept	-0.032 (±0.035)
R^2	0.938

3.3.7 $PM_{2.5}$ Mass Concentrations: Gravimetric vs. Continuous Measurements

Continuous monitoring of $PM_{2.5}$ concentrations were conducted at four monitoring sites by HKEPD during 2017. TEOMs (Tapered Element Oscillating Microbalance) are installed at MK and TW sites, while a Beta Attenuation Monitor (BAM-1020, Met One Instruments) and a Model 602 Beta^{PLUS} Particle Measurement System (Teledyne-API) are deployed for $PM_{2.5}$ monitoring at YL and KC sites, respectively. Comparisons of $PM_{2.5}$ mass concentrations from gravimetric measurement and 24-hr average TEOM/beta gauge measurement were conducted. The results are presented in both time-series plots and scatter plots (Figure 20). The two measurements show good agreement (R^2 = 0.95–0.97) with slopes ranging from 0.88 to 1.08.

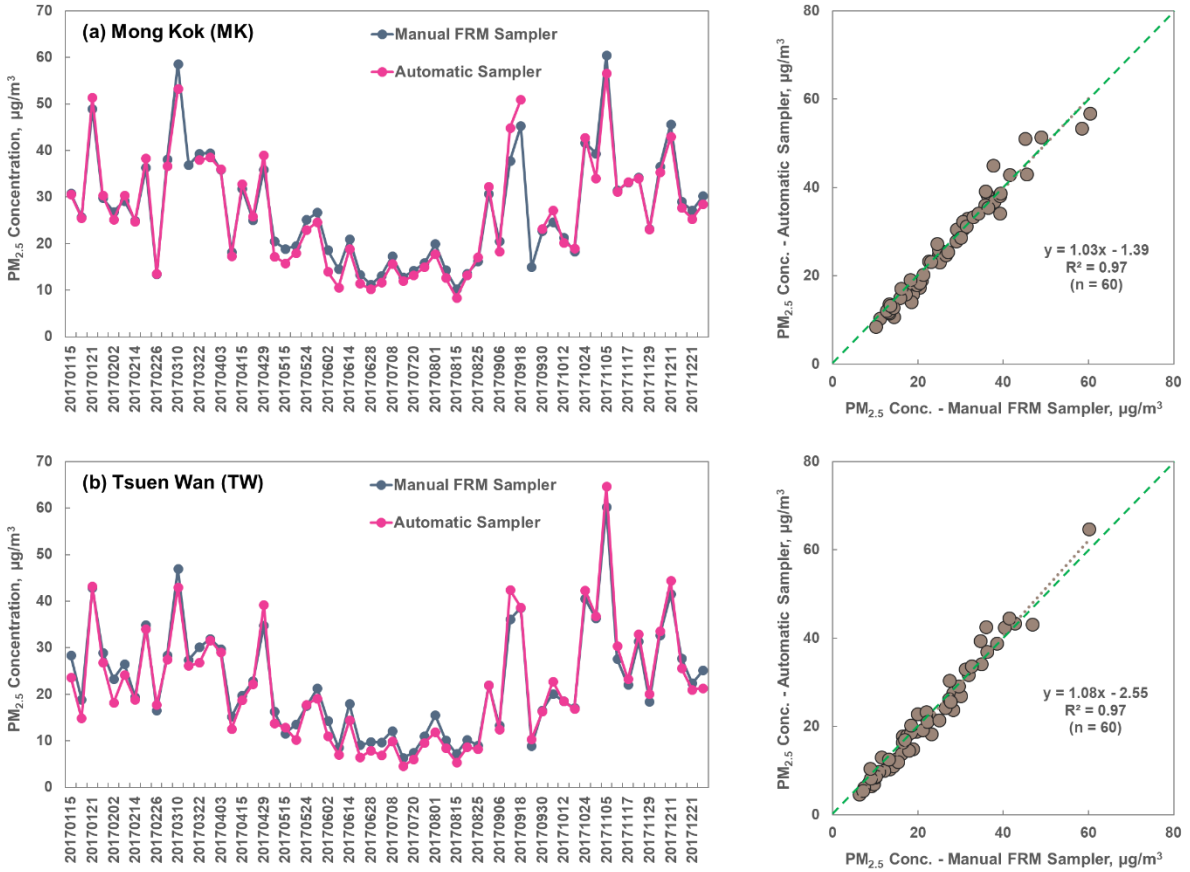

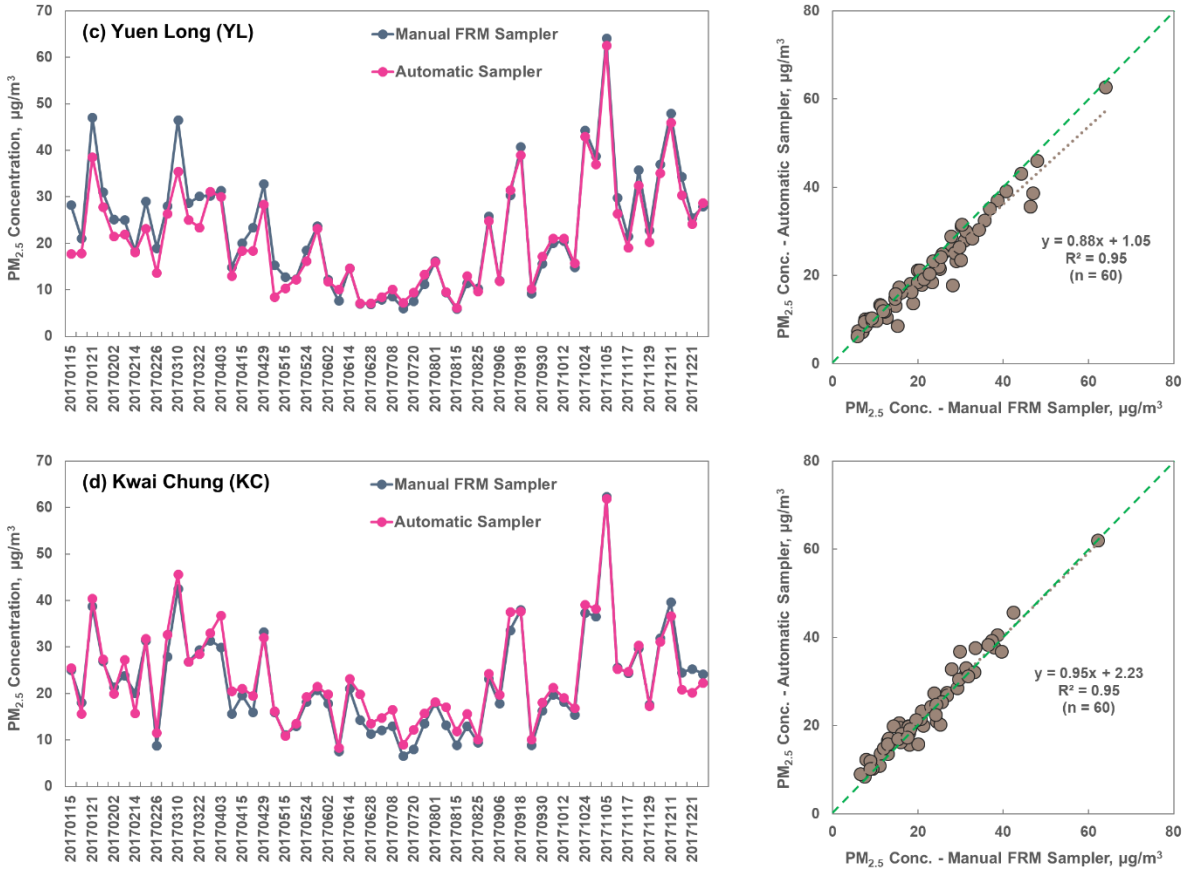

Figure 20. Comparisons of $PM_{2.5}$ mass concentrations from gravimetric and continuous measurements at (a) MK, (b) TW, (c) YL, and (d) KC sites during 2017.

4. $PM_{2.5}$ Annual Trend and Seasonal Variation

4.1 $PM_{2.5}$ Annual Trend

A side-by-side comparison of the annual average $PM_{2.5}$ concentration and chemical composition data is shown in Appendix A [Chow et al., 2002, 2006, 2010, 2016; Yu et al., 2012, 2013, 2014, 2015, 2017]. The MK and TW sites have data since 2000, the YL site has data since 2004, the WB site has data since 2011, the CW and TC sites have data during 2011–2016, the KC site started operation from May 2014, while no data is available from the Hok Tsui (HT) site after 2009.

Compared to the year of 2016, the annual average $PM_{2.5}$ concentrations at MK, WB, TW, and KC sites in 2017 fluctuated slightly upwards by 0.88-1.69 $\mu g/m^3$, corresponding to increase by 4%, 10%, 4%, and 6%, respectively; the annual average $PM_{2.5}$ concentration at YL site exhibited a decrease of 0.60 $\mu g/m^3$ or 3%.

Annual trends of $PM_{2.5}$ mass were examined for MK, WB, TW, and YL sites across the years when data are available (Figure 21). The Mann-Kendall non-parametric statistical test [Salmi et al., 2002; Sen, 1968] was applied to the dataset and shows a monotonic decreasing trend across all four sites since 2011. The Sen's slopes for annual average $PM_{2.5}$ concentrations are -2.95, -2.11, -2.34, and -2.13 $\mu g/m^3$/year at MK, WB, TW, and YL sites, respectively.

Measured species were grouped into nine categories for better comparison (Figure 22). For OC and EC at MK, TW, and YL sites, high concentration levels were observed in the first two studies (i.e. 2000–01 and 2004–05) and then the concentrations maintained at lower levels since 2008. At all four sites, the EC concentrations follow a broadly decline trend from 2011 to 2017 while the OC levels were comparable. For ammonium, sulfate, and nitrate, a quite clear decreasing trend could be observed across all four sites since 2011. For other species (i.e., geological material, sodium, potassium, and non-crustal trace elements), the concentrations were at similar levels all over the years.

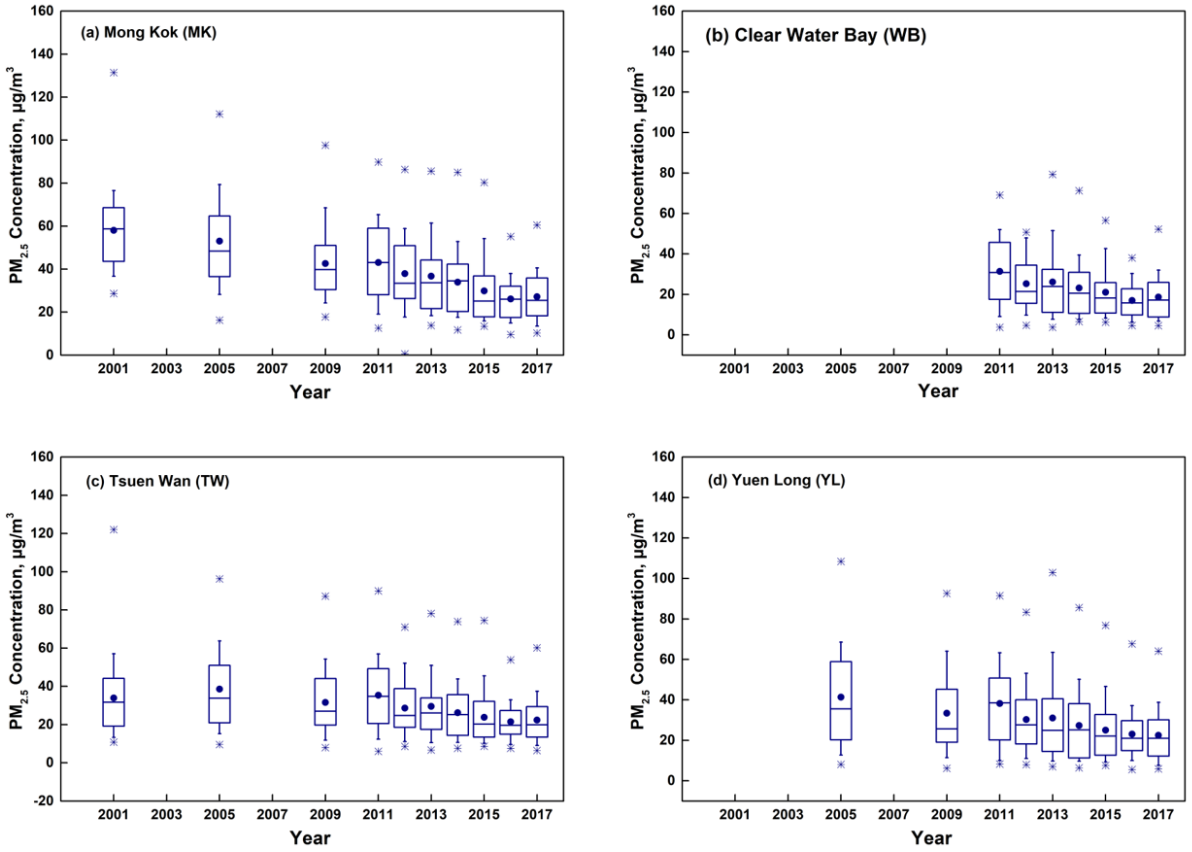

Figure 21. Comparisons of annual average $PM_{2.5}$ mass concentrations at (a) MK, (b) WB, (c) TW, and (d) YL sites from 2000 to 2017 (wherever data are available) (Bottom and top of box: the 25th and the 75th percentiles; whiskers: the 10th and 90th percentiles; dot in the box: the average; line in the box: the median; stars: the minimum and maximum values).

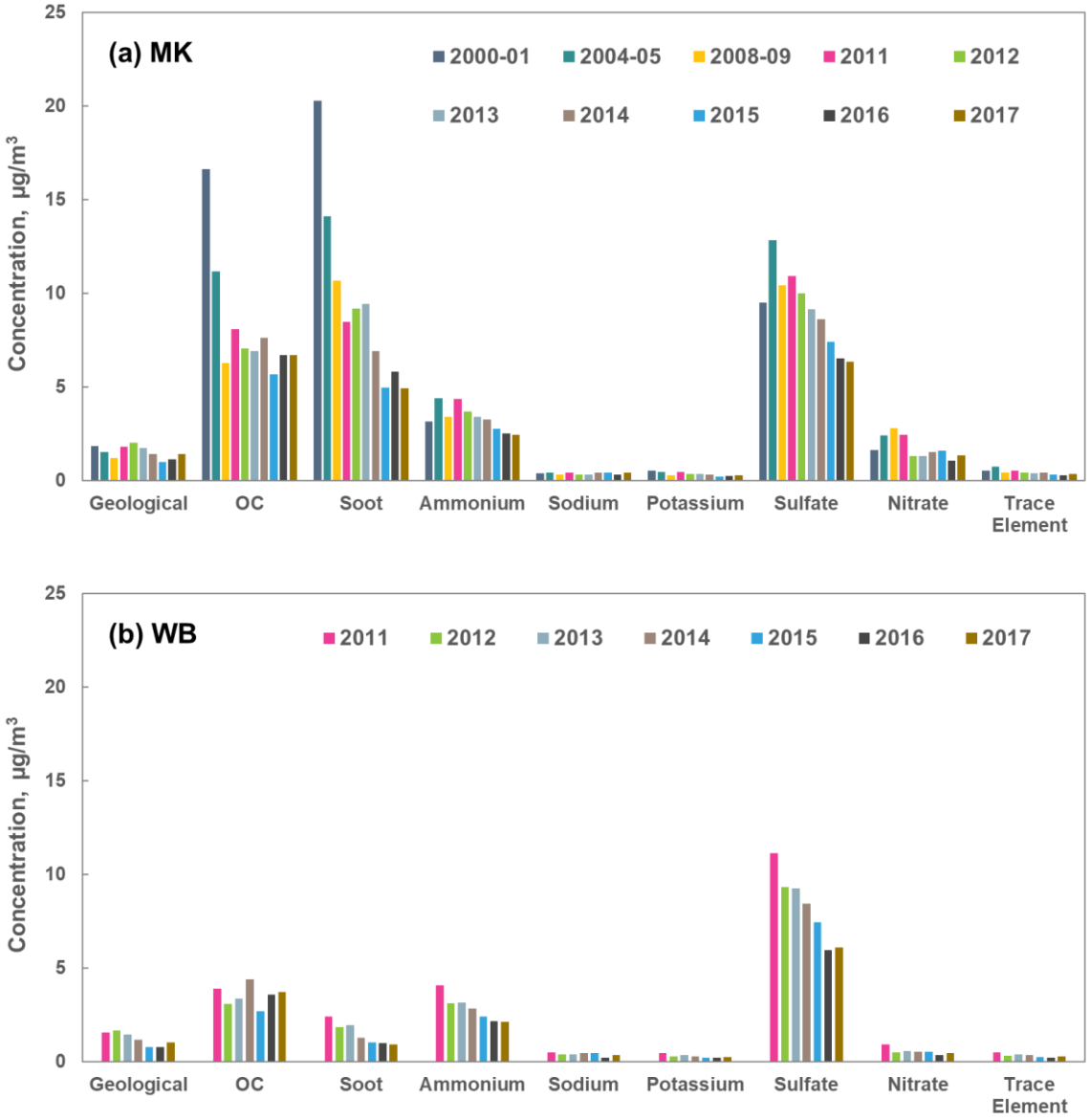
(a) MK
2000-01
2004-05
2008-09
2011
2012
2013
2014
2015
2016
2017
Concentration, µg/m3
25
20
15
10
5
0
Geological
OC
Soot
Ammonium
Sodium
Potassium
Sulfate
Nitrate
Trace Element
(b) WB
2011
2012
2013
2014
2015
2016
2017
Concentration, µg/m3
25
20
15
10
5
0
Geological
OC
Soot
Ammonium
Sodium
Potassium
Sulfate
Nitrate
Trace Element

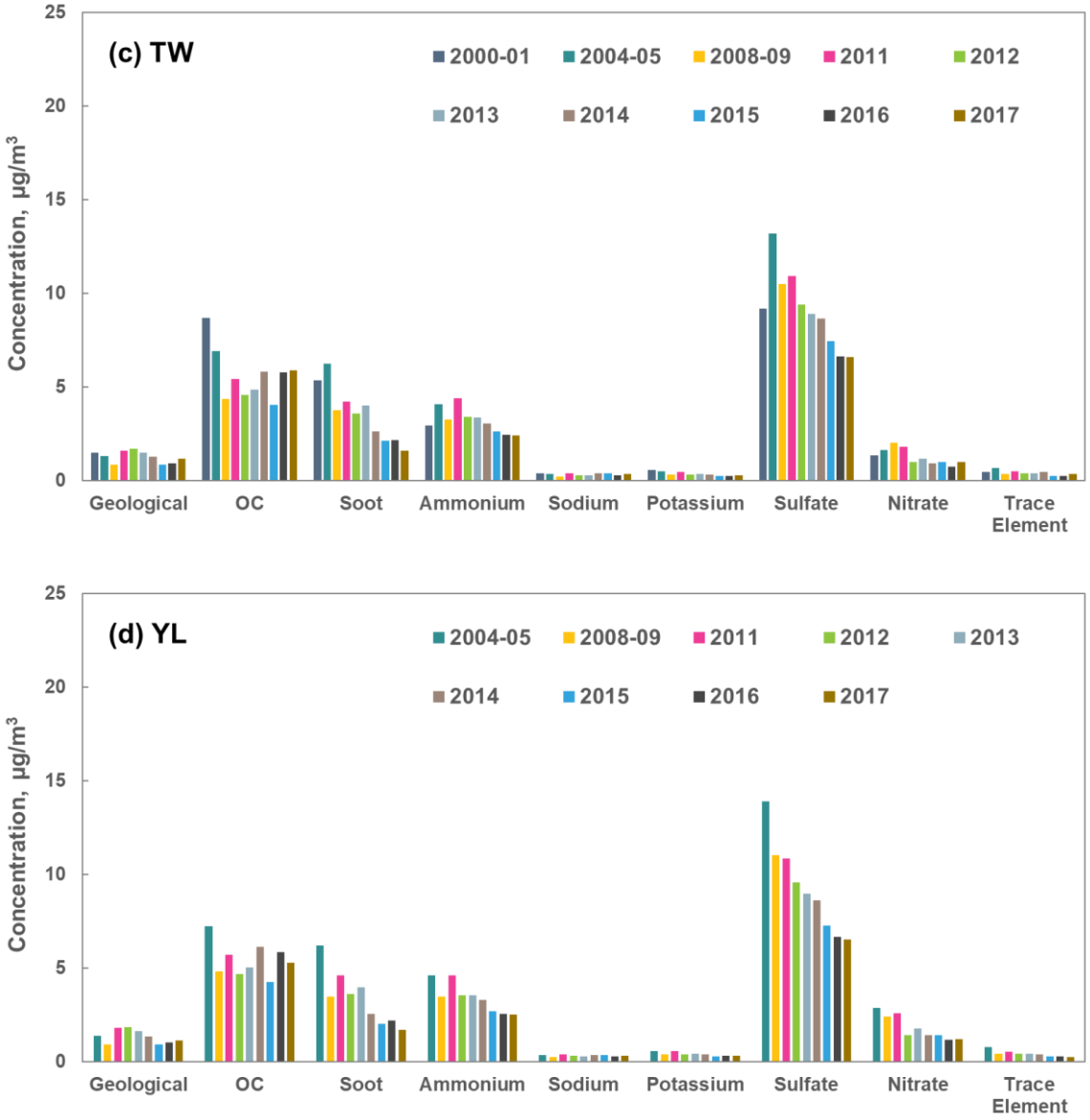

Figure 22. Annual trends of major components of $PM_{2.5}$ samples collected at (a) MK, (b) WB, (c) TW, and (e) YL sites from 2000 to 2017 (wherever data are available).

4.2 Seasonal Variation of $PM_{2.5}$ in 2017

Monthly average $PM_{2.5}$ concentration and chemical compositions for individual sites are shown in Figure 23. Higher $PM_{2.5}$ concentrations were recorded in January through March and December, primarily due to elevated levels of sulfate, nitrate, ammonium, and OM. The highest daily $PM_{2.5}$ concentration (64.08 μg/m^3) appeared at YL on November 5, 2017. On this day, KC experienced the second highest daily $PM_{2.5}$ (62.33 μg/m^3) while the other sites all had the highest daily $PM_{2.5}$. This result indicated a regional pollution episode brought in by northwesterly wind. The prevailing wind shifted from northwesterly in winter to southeasterly in summer, resulting in clean marine air diluting pollutants and improved air quality in the months of June and July.

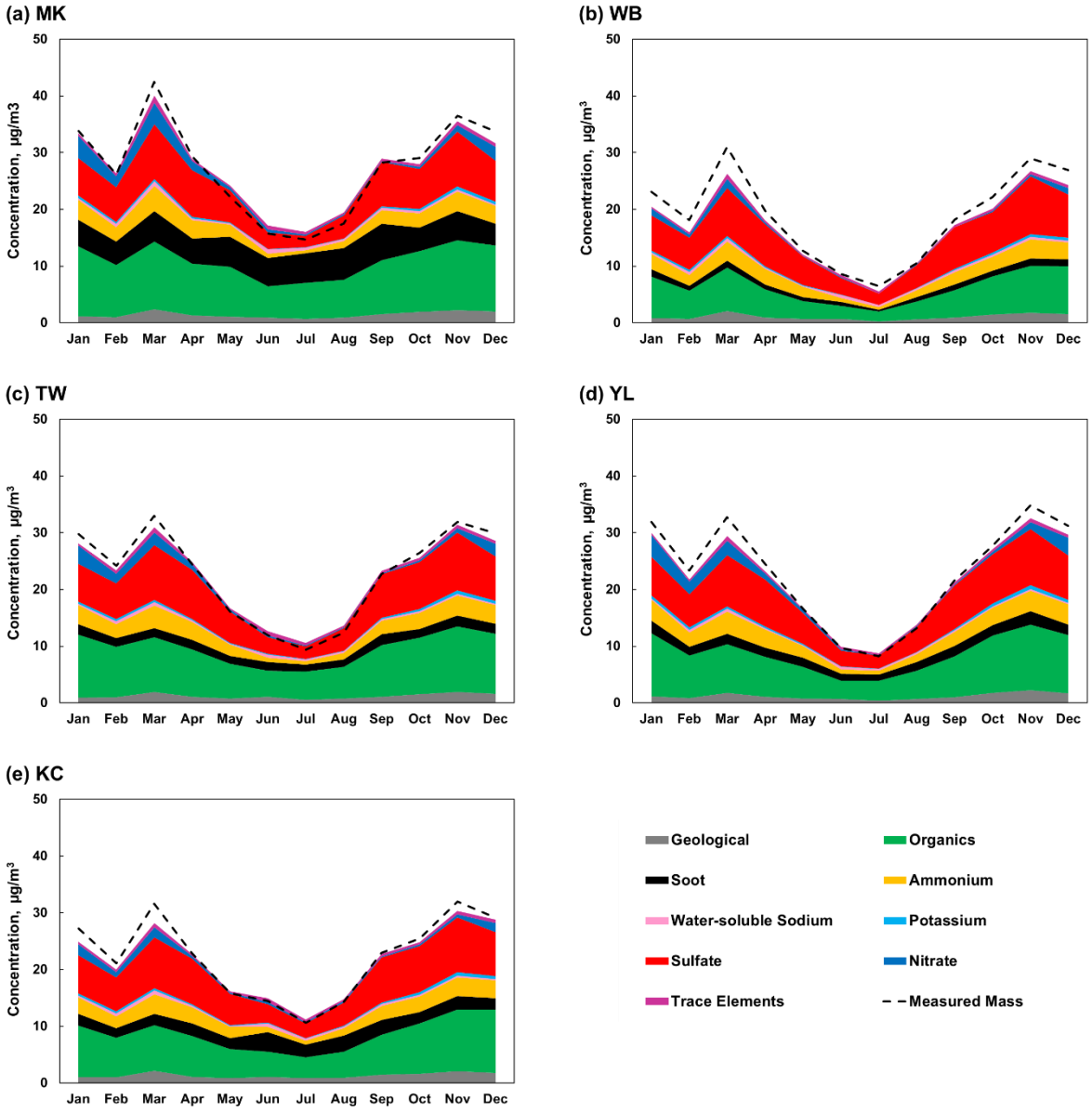

Figure 23. Monthly average of $PM_{2.5}$ mass concentrations and chemical compositions for (a) MK, (b) WB, (c) TW, (d) YL, and (e) KC during 2017 $PM_{2.5}$ speciation study.

5. Summary

This data summary report covers the validation and quality assurance aspects of the chemical analysis of filter samples from the Hong Kong $PM_{2.5}$ speciation network from January 1 through December 31, 2017. Sampling was conducted at MK, WB, TW, YL, and KC sites on a 1-in-6 day schedule which yielded a total of 60 sampling events through the year. Of the 792 $PM_{2.5}$ filter samples received, 791 $PM_{2.5}$ filter samples are considered valid after Level I data validation. Therefore, a total of 791 filters (719 $PM_{2.5}$ samples and 72 field blanks) were submitted for comprehensive chemical analyses.

The valid data rate exceeds 99%. One quartz filter sample collected at YL site on December 11, 2017 was flagged as invalid during sampling quality assurance process. The laboratory accuracy and precision were within limits as demonstrated by routine QC samples.

Three levels of validation were performed on the complete dataset. Reconstructed mass and measured mass were highly correlated with correlation coefficients (R^2) ranging from 0.98 to 0.99 at individual sites. It further supports the validity of both gravimetric analysis and chemical measurements. The reconstructed mass and the measured mass were in excellent agreement.

In 2017, the highest annual average $PM_{2.5}$ concentration of 27.18 $\mu g/m^3$ was measured at the roadside MK site. The lowest annual average $PM_{2.5}$ concentration of 18.67 $\mu g/m^3$ was found at the suburban WB site. The $PM_{2.5}$ concentrations at all the five monitoring sites were within the existing AQO annual $PM_{2.5}$ standard of 35 $\mu g/m^3$ and 24-hr average limit of 75 $\mu g/m^3$.

Similar to the past years, sulfate, formed from atmospheric oxidation of sulfur dioxide, is still the most abundant component in the $PM_{2.5}$ across all the five sites (23–33%). Organic carbon, with contributions from both primary emission sources (e.g., vehicular exhaust, biomass burning) and secondary formation from a myriad of volatile organic compound precursors, is the second most abundant component with mass contributions ranging from 20% at WB site to 26% at TW site. Organic matter, assuming to be 1.4×OC to account for non-carbon elements (e.g., O, N, S, H), had mass contributions ranging from 28% at WB to 37% at TW. Nitrate, formed from atmospheric oxidation of nitrogen oxides, was much lower than sulfate, contributing 3–5% to the total fine PM masses at all the sampling sites. Ammonium, coming from ammonia (the most abundant alkaline gas in the atmosphere), was reasonably balanced by sulfate and nitrate and it was suggested to exist dominantly as ammonium sulfate across all the sampling sites in the year of 2017. EC, exclusively from combustion sources, exhibited a clear roadside-urban-suburban gradient pattern with the highest annual average concentration (4.95 $\mu gC/m^3$, 18% of the $PM_{2.5}$ mass) observed at MK site and the lowest annual average concentration (1.60 $\mu gC/m^3$, 5% of the $PM_{2.5}$ mass) at WB site.

Hong Kong experienced higher $PM_{2.5}$ levels during fall and winter months (Jan, Feb, Mar, Oct, Nov, and Dec) while summer months (Jun–Aug) usually have lower $PM_{2.5}$ concentrations. The extra mass between the high and low $PM_{2.5}$ concentrations was mainly attributed to $(NH_4)_2SO_4$ and organics which usually exhibited high concentrations simultaneously across all five sites, suggesting that regional sources were the most probable $PM_{2.5}$ contributors on high $PM_{2.5}$ concentration days. On the other hand, the lack of temporal variation for EC concentrations at individual site, together with the aforementioned roadside-urban-suburban gradient pattern, suggested that local sources (e.g. on-road vehicles) were its major contributors. While a wide range of measures taken by the HKSAR Government to control the vehicular emissions have proved to be effective and responsible for the general decreasing trend of EC levels observed

at roadside, continuous efforts are needed to contain the air pollution at lower levels so as to keep compliance with the existing AQO criteria.

Moreover, the meteorological conditions (especially wind speed and direction) have a large influence on the PM levels measured in Hong Kong. Lower $PM_{2.5}$ concentrations were observed during June–August when the southerly winds prevailed and brought in clean maritime air while higher $PM_{2.5}$ concentrations were usually associated with northeasterly winds which carried regional pollutants into Hong Kong.

Compared to the year of 2016, the annual average $PM_{2.5}$ concentrations at MK, WB, TW, and KC sites in 2017 fluctuated slightly upwards by 0.88-1.69 $\mu g/m^3$, corresponding to increase by 4%, 10%, 4%, and 6%, respectively; the annual average $PM_{2.5}$ concentration at YL site exhibited a decrease of 0.60 $\mu g/m^3$ or 3%. The Mann-Kendall non-parametric statistical test showed a continuing downward trend in overall $PM_{2.5}$ concentrations in Hong Kong over the past decade, indicating that the general air quality in Hong Kong is improving.

References

Bevington, P. R. (1969), Data Reduction and Error Analysis for the Physical Sciences, MaGraw Hill, New York, NY.

Birch, M. E. and R. A. Cary (1996), Elemental carbon-based method for monitoring occupational exposures to particulate diesel exhaust, *Aerosol Sci. Technol.*, 25, 221-241.

Chen, L. -W. A., J. C. Chow, J. G. Watson, H. Moosmüller, and W. P. Arnott (2004), Modeling reflectance and transmittance of quartz-fiber filter samples containing elemental carbon particles: Implications for thermal/optical analysis, *J. Aerosol Sci.*, 35, 765-780.

Chow, J. C., J. G. Watson, L. C. Pritchett, W. R. Pierson, C. A. Frazier, and R. G. Purcell (1993), The DRI thermal/optical reflectance carbon analysis system: description, evaluation and applications in U. S. air quality studies, *Atmos. Environ.*, 27A, 1185-1201.

Chow, J. C., J. G. Watson, L. -W. A. Chen, W. P. Arnott, H. Moosmüller, and K. K. Fung (2004), Equivalence of elemental carbon by Thermal/Optical Reflectance and Transmittance with different temperature protocols, *Environ. Sci. Technol.*, 38, 4414-4422.

Chow, J. C., J. G. Watson, L. -W. A. Chen, M. C. O. Chang, N. F. Robinson, D. Trimble, and S. D. Kohl (2007), The IMPROVE_A temperature protocol for thermal/optical carbon analysis: maintaining consistency with a long-term database, *J. Air Waste Manage. Assoc.*, 57, 1014-1023.

Chow, J. C., J. G. Watson, Kohl, S. D., Gonzi, M. P., L. -W. A. Chen (2002), Measurements and Validation for the Twelve Month Particulate Matter Study in Hong Kong, available at: http://www.epd.gov.hk/epd/english/environmentinhk/air/studyrpts/files/final_version_hkepdfinalreport_rev12-12-02.pdf.

Chow, J. C., J. G. Watson, Kohl, S. D., Voepel, H. E., L. -W. A. Chen (2006), Measurements and Validation for the Twelve Month Particulate Matter Study in Hong Kong, available at: http://www.epd.gov.hk/epd/english/environmentinhk/air/studyrpts/files/HKEPDFinalReportRev_V8.pdf.

Chow, J. C., J. G. Watson, Kohl, S. D., L. -W. A. Chen (2010), Measurements and validation of the 2008/2009 particulate matter study in Hong Kong, available at: http://www.epd.gov.hk/epd/english/environmentinhk/air/studyrpts/files/HKEPDFinalReportRev_11-29-10_v2.pdf.

Chow, J. F., J. G. Watson, P. M. Cropper, X. Wang, and S. D. Kohl (2016), Fine Particulate Matter ($PM_{2.5}$) Sample Chemical Analysis January 1, 2015 – December 31, 2015, available at HKEPD website: http://www.epd.gov.hk/epd/sites/default/files/epd/english/environmentinhk/air/studyrpts/files/final_report_mvtmpms_2015.pdf.

Hong Kong Observatory (HKO) (2013), The year's weather – 2013, Climatological Publications, available at: http://www.weather.gov.hk/wxinfo/pastwx/ywx2013.htm.

Research Triangle Institute (RTI) (2005), Data validation process for the $PM_{2.5}$ Chemical Speciation Network, Prepared for Center for Environmental Measurements and Quality Assurance, USEPA.

Salmi, T., A. Määttä, P. Anttila, T. Ruoho-Airola, and T. Amnell (2002), Detecting trends of annual values of atmospheric pollutants by the Mann-Kendall test and Sen's slope estimates – the excel template application MAKESENS, Finnish Meteorological Institute, Helsinki.

Sen, P. K. (1968), Estimates of the regression coefficient based on Kendall's Tau, *J. Am. Stat. Assoc.*, 63, 1379-1389.

U. S. Environmental Protection Agency (USEPA) (1999), Particulate Matter ($PM_{2.5}$) Speciation Guidance, available at: http://www.epa.gov/ttnamti1/files/ambient/pm25/spec/specfinl.pdf.

U. S. Environmental Protection Agency (USEPA) (2012), Quality Assurance Guidance Document for $PM_{2.5}$ Chemical Speciation Sampling at Trends, NCore, Supplemental and Tribal Sites, available at: http://www.epa.gov/ttnamti1/files/ambient/pm25/spec/CSN_QAPP_v120_05-2012.pdf.

Watson, J. G., J. C. Chow, and C. A. Frazier (1999), X-ray fluorescence analysis of ambient air samples, Elemental Analysis of Airborne Particles, Vol 1, by S. Landsberger and M. Creatchman, Eds. Gordon and Breach Science, Amsterdam, 67-96.

Watson, J. G., B. J. Turpin, and J. C. Chow (2001), The measurement process: Precision, accuracy, and validity, in *Air Sampling Instrument for Evaluation for Atmospheric Contaminants*, 9th ed., B. S. Cohen and C. S. J. McCammon, Eds. American Conference of Governmental Industrial Hygienists, Cincinnati, OH, 201-216.

Witz, S., R. W. Eden, M. W. Wadley, C. Dunwoody, R. P. Papa, and K. J. Torre (1990), Rapid loss of particulate nitrate, chloride and ammonium on quartz fiber filters during storage, *J. Air Waste Manage. Assoc.*, 40, 53-61.

Yu, J. Z., X. H. H. Huang, and W. M. Ng (2012), Final report for provision of service for fine particulate matter ($PM_{2.5}$) sample chemical analysis, available at HKEPD website: http://www.epd.gov.hk/epd/english/environmentinhk/air/studyrpts/files/final_report_mvtmpms_2011.pdf.

Yu, J. Z., X. H. H. Huang, and W. M. Ng (2013), Final report for provision of service for fine particulate matter ($PM_{2.5}$) sample chemical analysis, available at HKEPD website: http://www.epd.gov.hk/epd/english/environmentinhk/air/studyrpts/files/final_report_mvtmpms_2012.pdf.

Yu, J. Z., X. H. H. Huang, T. Zhang, and W. M. Ng (2014), Final report for chemical speciation of $PM_{2.5}$ filter samples, January 1 through December 31, 2013, available at HKEPD website: http://www.epd.gov.hk/epd/sites/default/files/epd/english/environmentinhk/air/studyrpts/files/final_report_mvtmpms_2013.pdf.

Yu, J. Z. and T. Zhang (2017), Final report for chemical speciation of $PM_{2.5}$ filter samples, January 1 through December 31, 2016, available at HKEPD website: http://www.epd.gov.hk/epd/sites/default/files/epd/english/environmentinhk/air/studyrpts/files/final_report_mvtmpms_2016.pdf.

Appendix A. Annual average $PM_{2.5}$ concentration and chemical composition measured in Hong Kong during 2000–2017.

	MK										WB						
	2000-01	2004-05	2008-09	2011	2012	2013	2014	2015	2016	2017	2011	2012	2013	2014	2015	2016	2017
Teflon Mass	58.28	53.02	41.60	43.08	38.93	36.72	33.90	29.82	26.11	27.18	31.32	25.48	26.08	23.12	21.08	16.98	18.67
Quartz Mass	62.50	54.87	45.92	47.92	58.03	41.38	35.99	32.42	27.95	29.79	35.89	45.58	30.38	23.81	22.37	17.10	19.32
Cl^-	0.256	0.283	0.312	0.205	0.102	0.119	0.203	0.226	0.114	0.191	0.105	0.067	0.093	0.123	0.082	0.035	0.072
NO_3^-	1.653	2.404	2.809	2.452	1.321	1.313	1.528	1.600	1.082	1.356	0.934	0.508	0.580	0.520	0.530	0.347	0.469
SO_4^{2-}	9.50	12.84	10.41	10.91	10.01	9.14	8.60	7.42	6.53	6.36	11.13	9.34	9.25	8.45	7.45	5.97	6.12
NH_4^+	3.17	4.40	3.40	4.37	3.68	3.42	3.28	2.75	2.51	2.45	4.09	3.13	3.16	2.85	2.40	2.16	2.12
Na^+	0.398	0.423	0.320	0.431	0.324	0.326	0.420	0.426	0.326	0.439	0.510	0.394	0.401	0.482	0.454	0.211	0.376
K^+	0.457	0.479	0.278	0.467	0.349	0.319	0.286	0.190	0.223	0.235	0.483	0.288	0.318	0.273	0.181	0.194	0.209
OC	16.64	11.18	6.26	8.09	7.05	6.92	7.64	5.67	6.72	6.72	3.91	3.07	3.37	4.39	2.71	3.57	3.73
EC	20.29	14.12	10.66	8.48	9.20	9.42	6.91	4.96	5.83	4.95	2.43	1.84	1.96	1.29	1.02	1.01	0.93
TC	36.91	25.28	16.91	16.55	16.25	16.33	14.54	10.62	12.55	11.66	6.31	4.92	5.33	5.68	3.72	4.58	4.66
Al	0.1139	0.1408	0.0986	0.1942	0.2365	0.2034	0.1671	0.0885	0.1220	0.1472	0.1990	0.2260	0.2005	0.1686	0.0943	0.1117	0.1348
Si	0.4778	0.3469	0.2485	0.3981	0.4393	0.3732	0.2760	0.1604	0.1993	0.2680	0.3980	0.4064	0.3527	0.2690	0.1577	0.1739	0.2369
P	0.0092	0.1886	0.0225	0.0194	0.0211	0.0177	0.0188	0.0000	0.0044	0.0041	0.0150	0.0129	0.0124	0.0134	0.0000	0.0017	0.0025
S	3.4886	4.3005	3.3471	3.6677	3.3455	3.1377	3.0873	2.8024	2.5718	2.5841	3.8399	3.1763	3.2338	3.0280	2.8453	2.3997	2.4413
Cl	0.1169	0.1391	0.1037	0.0889	0.0386	0.0754	0.1303	0.1299	0.0620	0.1466	0.0720	0.0235	0.0954	0.1324	0.0739	0.0440	0.1047
K	0.5517	0.4678	0.3064	0.4619	0.3447	0.3658	0.3136	0.2329	0.2464	0.3008	0.4740	0.3005	0.3690	0.3030	0.2297	0.2221	0.2672
Ca	0.1705	0.1082	0.1102	0.1298	0.1461	0.1244	0.1061	0.1049	0.0959	0.1216	0.0914	0.1090	0.0853	0.0722	0.0752	0.0518	0.0769
Ti	0.0092	0.0109	0.0109	0.0128	0.0147	0.0126	0.0099	0.0086	0.0086	0.0103	0.0106	0.0116	0.0103	0.0078	0.0079	0.0058	0.0072
V	0.0134	0.0190	0.0175	0.0146	0.0197	0.0219	0.0263	0.0167	0.0178	0.0149	0.0119	0.0133	0.0145	0.0148	0.0131	0.0144	0.0122
Cr	0.0010	0.0017	0.0014	0.0021	0.0023	0.0022	0.0021	0.0021	0.0008	0.0028	0.0022	0.0019	0.0017	0.0018	0.0015	0.0005	0.0015
Mn	0.0128	0.0170	0.0127	0.0214	0.0194	0.0163	0.0132	0.0093	0.0084	0.0107	0.0174	0.0132	0.0130	0.0103	0.0073	0.0048	0.0074
Fe	0.2692	0.2579	0.2343	0.2958	0.3051	0.2779	0.2538	0.2447	0.2547	0.2881	0.1582	0.1527	0.1344	0.1207	0.1110	0.0822	0.1154
Co	0.0001	0.0001	0.0002	0.0005	0.0002	0.0002	0.0007	0.0000	0.0004	0.0002	0.0003	0.0001	0.0001	0.0002	0.0000	0.0001	0.0000
Ni	0.0055	0.0061	0.0049	0.0050	0.0065	0.0068	0.0070	0.0049	0.0048	0.0042	0.0042	0.0045	0.0052	0.0042	0.0042	0.0038	0.0037
Cu	0.0113	0.0110	0.0210	0.0252	0.0214	0.0230	0.0217	0.0210	0.0137	0.0175	0.0225	0.0177	0.0203	0.0159	0.0101	0.0106	0.0153
Zn	0.1794	0.2399	0.1579	0.2156	0.1887	0.1567	0.1347	0.0957	0.0869	0.1045	0.1948	0.1337	0.1397	0.1062	0.0741	0.0572	0.0761
Ga	0.0004	0.0018	0.0003	0.0003	0.0001	0.0000	0.0001	0.0000	0.0004	0.0000	0.0002	0.0002	0.0002	0.0001	0.0000	0.0001	0.0002
As	0.0046	0.0053	0.0012	0.0043	0.0030	0.0035	0.0019	0.0028	0.0001	0.0005	0.0053	0.0026	0.0040	0.0023	0.0035	0.0002	0.0007
Se	0.0021	0.0003	0.0003	0.0000	0.0000	0.0000	0.0000	0.0010	0.0000	0.0000	0.0000	0.0000	0.0000	0.0000	0.0010	0.0000	0.0000
Br	0.0129	0.0106	0.0172	0.0172	0.0132	0.0129	0.0132	0.0110	0.0060	0.0109	0.0190	0.0160	0.0158	0.0144	0.0127	0.0056	0.0112
Rb	0.0036	0.0020	0.0010	0.0011	0.0007	0.0007	0.0000	0.0009	0.0006	0.0007	0.0014	0.0006	0.0005	0.0001	0.0008	0.0004	0.0003
Sr	0.0013	0.0011	0.0017	0.0030	0.0018	0.0020	0.0008	0.0018	0.0010	0.0006	0.0030	0.0016	0.0020	0.0007	0.0019	0.0010	0.0007
Y	0.0001	0.0004	0.0003	0.0002	0.0001	0.0001	0.0001	0.0003	0.0001	0.0000	0.0004	0.0000	0.0001	0.0001	0.0003	0.0001	0.0000
Zr	0.0006	0.0016	0.0010	0.0006	0.0014	0.0004	0.0005	0.0013	0.0004	0.0012	0.0003	0.0006	0.0006	0.0006	0.0007	0.0002	0.0007
Mo	0.0005	0.0015	0.0007	0.0016	0.0001	0.0000	0.0021	0.0011	0.0026	0.0000	0.0011	0.0001	0.0000	0.0014	0.0005	0.0015	0.0000
Pd	0.0012	0.0019	0.0006	0.0016	0.0000	0.0000	0.0001	0.0005	0.0003	0.0000	0.0023	0.0000	0.0000	0.0001	0.0002	0.0001	0.0000
Ag	0.0011	0.0013	0.0010	0.0003	0.0000	0.0003	0.0000	0.0000	0.0001	0.0002	0.0003	0.0003	0.0002	0.0000	0.0001	0.0001	0.0004
Cd	0.0019	0.0022	0.0008	0.0006	0.0007	0.0002	0.0005	0.0004	0.0005	0.0003	0.0005	0.0007	0.0005	0.0001	0.0004	0.0002	0.0000
In	0.0018	0.0009	0.0005	0.0003	0.0001	0.0000	0.0001	0.0002	0.0004	0.0006	0.0005	0.0000	0.0000	0.0000	0.0001	0.0003	0.0007
Sn	0.0188	0.0131	0.0107	0.0131	0.0041	0.0034	0.0032	0.0025	0.0055	0.0016	0.0125	0.0035	0.0046	0.0038	0.0017	0.0045	0.0020
Sb	0.0046	0.0042	0.0009	0.0080	0.0005	0.0005	0.0021	0.0007	0.0008	0.0002	0.0068	0.0007	0.0006	0.0015	0.0005	0.0012	0.0004
Ba	0.0267	0.0106	0.0031	0.0167	0.0348	0.0109	0.0042	0.0003	0.0194	0.0142	0.0087	0.0127	0.0048	0.0039	0.0005	0.0150	0.0065
La	0.0131	0.0105	0.0036	0.0164	0.0000	0.0000	0.0040	0.0008	0.0190	0.0024	0.0146	0.0000	0.0000	0.0041	0.0014	0.0137	0.0013
Au	0.0003	0.0003	0.0000	0.0000	0.0000	0.0002	0.0001	0.0001	0.0000	0.0000	0.0000	0.0001	0.0001	0.0000	0.0001	0.0000	0.0000
Hg	0.0001	0.0000	0.0000	0.0000	0.0000	0.0000	0.0000	0.0000	0.0000	0.0000	0.0000	0.0000	0.0000	0.0000	0.0001	0.0000	0.0000
Tl	0.0001	0.0002	0.0000	0.0000	0.0000	0.0000	0.0001	0.0000	0.0001	0.0000	0.0000	0.0000	0.0000	0.0002	0.0000	0.0000	0.0000
Pb	0.0664	0.0478	0.0405	0.0597	0.0399	0.0383	0.0317	0.0182	0.0161	0.0182	0.0626	0.0370	0.0413	0.0344	0.0181	0.0173	0.0189
U	0.0001	0.0013	0.0008	0.0040	0.0001	0.0000	0.0001	0.0002	0.0000	0.0000	0.0040	0.0000	0.0000	0.0002	0.0002	0.0000	0.0000

	TW										YL								
	2000-01	2004-	2008-09	2011	2012	2013	2014	2015	2016	2017	2004-05	2008-09	2011	2012	2013	2014	2015	2016	2017
Teflon Mass	34.12	38.59	30.61	35.30	28.64	29.50	26.19	23.83	21.50	22.38	41.31	31.78	38.22	30.15	31.01	27.29	25.02	23.10	22.50
Quartz Mass	37.28	40.75	34.00	40.56	48.26	33.97	28.66	26.34	22.91	24.75	43.91	36.34	42.89	50.23	35.37	29.80	26.70	23.96	24.21
Cl^-	0.138	0.126	0.175	0.122	0.082	0.095	0.138	0.130	0.084	0.113	0.264	0.213	0.174	0.131	0.111	0.142	0.093	0.104	0.107
NO_3^-	1.343	1.635	2.031	1.795	1.015	1.173	0.933	1.006	0.756	0.993	2.864	2.419	2.590	1.434	1.761	1.431	1.429	1.161	1.213
SO_4^{2-}	9.17	13.17	10.48	10.91	9.41	8.88	8.66	7.45	6.62	6.60	13.91	11.04	10.85	9.58	8.96	8.63	7.28	6.66	6.52
NH_4^+	2.96	4.07	3.27	4.38	3.40	3.36	3.05	2.63	2.44	2.41	4.62	3.47	4.63	3.56	3.54	3.29	2.71	2.57	2.52
Na^+	0.397	0.362	0.211	0.404	0.306	0.292	0.398	0.379	0.307	0.371	0.375	0.262	0.402	0.323	0.278	0.352	0.344	0.274	0.322
K^+	0.492	0.486	0.308	0.492	0.318	0.309	0.294	0.186	0.221	0.235	0.562	0.365	0.590	0.374	0.385	0.348	0.234	0.298	0.260
OC	8.69	6.93	4.38	5.44	4.57	4.86	5.83	4.05	5.78	5.90	7.23	4.83	5.73	4.69	5.02	6.15	4.24	5.85	5.29
EC	5.37	6.26	3.76	4.24	3.59	4.01	2.61	2.15	2.18	1.60	6.19	3.49	4.61	3.60	3.96	2.57	2.04	2.22	1.70
TC	14.04	13.18	8.12	9.65	8.16	8.86	8.45	6.20	7.96	7.50	13.42	8.31	10.31	8.29	8.97	8.72	6.28	8.07	6.99
Al	0.1146	0.1414	0.0828	0.1910	0.2118	0.1916	0.1676	0.0864	0.1190	0.1399	0.1448	0.0913	0.2114	0.2368	0.2115	0.1784	0.0903	0.1299	0.1389
Si	0.3870	0.3141	0.1853	0.3888	0.3899	0.3436	0.2728	0.1572	0.1875	0.2474	0.3221	0.2073	0.4349	0.4311	0.3779	0.2897	0.1726	0.2040	0.2413
P	0.0050	0.1950	0.0237	0.0163	0.0138	0.0140	0.0157	0.0000	0.0023	0.0030	0.1917	0.0229	0.0155	0.0148	0.0145	0.0137	0.0000	0.0020	0.0022
S	3.3789	4.5835	3.4305	3.7641	3.1509	3.1369	3.0678	2.8011	2.5678	2.5679	4.5622	3.4535	3.7813	3.2280	3.0990	3.0908	2.7812	2.5303	2.5762
Cl	0.0874	0.0758	0.0568	0.0640	0.0491	0.0741	0.0947	0.0563	0.0501	0.1232	0.1590	0.0941	0.0774	0.0621	0.0788	0.0941	0.0683	0.0640	0.0917
K	0.5858	0.5080	0.3281	0.4797	0.3211	0.3622	0.3194	0.2363	0.2461	0.2909	0.5631	0.3828	0.5722	0.3882	0.4366	0.3839	0.2850	0.3290	0.3227
Ca	0.1262	0.0896	0.0729	0.1006	0.1253	0.1053	0.0993	0.0932	0.0758	0.1048	0.0891	0.0738	0.1111	0.1207	0.1088	0.0935	0.0938	0.0802	0.0878
Ti	0.0088	0.0102	0.0084	0.0117	0.0127	0.0106	0.0093	0.0081	0.0074	0.0085	0.0114	0.0097	0.0156	0.0153	0.0139	0.0108	0.0093	0.0093	0.0117
V	0.0137	0.0237	0.0182	0.0206	0.0208	0.0245	0.0258	0.0228	0.0213	0.0157	0.0195	0.0144	0.0139	0.0145	0.0142	0.0176	0.0147	0.0160	0.0132
Cr	0.0009	0.0015	0.0012	0.0021	0.0022	0.0017	0.0021	0.0019	0.0003	0.0018	0.0017	0.0016	0.0024	0.0022	0.0020	0.0023	0.0021	0.0003	0.0017
Mn	0.0124	0.0158	0.0113	0.0186	0.0163	0.0156	0.0155	0.0094	0.0071	0.0104	0.0170	0.0127	0.0215	0.0190	0.0183	0.0140	0.0102	0.0102	0.0103
Fe	0.1871	0.1858	0.1325	0.1932	0.1962	0.1780	0.1802	0.1626	0.1467	0.1760	0.1996	0.1552	0.2215	0.2223	0.2027	0.1877	0.1752	0.1657	0.1785
Co	0.0001	0.0001	0.0002	0.0003	0.0001	0.0001	0.0002	0.0000	0.0002	0.0001	0.0001	0.0001	0.0004	0.0001	0.0000	0.0003	0.0000	0.0002	0.0001
Ni	0.0054	0.0071	0.0052	0.0064	0.0113	0.0073	0.0068	0.0065	0.0056	0.0044	0.0068	0.0044	0.0049	0.0051	0.0049	0.0051	0.0045	0.0041	0.0037
Cu	0.0090	0.0104	0.0188	0.0207	0.0151	0.0212	0.0182	0.0123	0.0092	0.0117	0.0113	0.0167	0.0234	0.0167	0.0378	0.0321	0.0127	0.0110	0.0112
Zn	0.1743	0.2186	0.1343	0.1936	0.1704	0.1501	0.2017	0.0828	0.0758	0.1175	0.2381	0.1600	0.2188	0.1879	0.1515	0.1183	0.1052	0.0963	0.0782
Ga	0.0004	0.0030	0.0004	0.0001	0.0000	0.0000	0.0001	0.0000	0.0001	0.0003	0.0024	0.0003	0.0001	0.0002	0.0001	0.0000	0.0000	0.0001	0.0002
As	0.0055	0.0063	0.0010	0.0046	0.0029	0.0038	0.0020	0.0027	0.0002	0.0005	0.0084	0.0016	0.0058	0.0029	0.0044	0.0022	0.0035	0.0005	0.0004
Se	0.0022	0.0004	0.0004	0.0000	0.0001	0.0000	0.0000	0.0009	0.0000	0.0000	0.0005	0.0004	0.0000	0.0000	0.0001	0.0000	0.0010	0.0000	0.0000
Br	0.0127	0.0099	0.0148	0.0156	0.0108	0.0128	0.0115	0.0104	0.0059	0.0096	0.0116	0.0143	0.0171	0.0122	0.0133	0.0123	0.0105	0.0060	0.0089
Rb	0.0043	0.0025	0.0011	0.0014	0.0006	0.0006	0.0003	0.0009	0.0006	0.0004	0.0029	0.0015	0.0016	0.0010	0.0008	0.0005	0.0012	0.0008	0.0007
Sr	0.0011	0.0011	0.0019	0.0029	0.0015	0.0015	0.0007	0.0017	0.0009	0.0006	0.0015	0.0020	0.0030	0.0014	0.0017	0.0006	0.0017	0.0013	0.0008
Y	0.0001	0.0004	0.0004	0.0003	0.0001	0.0001	0.0001	0.0004	0.0001	0.0000	0.0004	0.0003	0.0004	0.0001	0.0001	0.0001	0.0002	0.0002	0.0000
Zr	0.0006	0.0013	0.0008	0.0004	0.0005	0.0007	0.0008	0.0008	0.0005	0.0003	0.0007	0.0011	0.0006	0.0007	0.0006	0.0011	0.0010	0.0004	0.0010
Mo	0.0005	0.0011	0.0006	0.0013	0.0002	0.0000	0.0018	0.0007	0.0011	0.0000	0.0017	0.0007	0.0009	0.0001	0.0000	0.0027	0.0007	0.0015	0.0000
Pd	0.0017	0.0014	0.0007	0.0019	0.0000	0.0000	0.0001	0.0004	0.0009	0.0000	0.0016	0.0008	0.0018	0.0000	0.0000	0.0001	0.0003	0.0005	0.0000
Ag	0.0017	0.0020	0.0007	0.0001	0.0004	0.0002	0.0000	0.0002	0.0000	0.0002	0.0018	0.0008	0.0001	0.0002	0.0003	0.0000	0.0001	0.0001	0.0001
Cd	0.0023	0.0021	0.0007	0.0004	0.0010	0.0006	0.0001	0.0005	0.0005	0.0004	0.0025	0.0007	0.0007	0.0008	0.0004	0.0005	0.0003	0.0003	0.0003
In	0.0020	0.0010	0.0005	0.0003	0.0000	0.0000	0.0000	0.0001	0.0006	0.0005	0.0017	0.0005	0.0002	0.0001	0.0000	0.0000	0.0001	0.0005	0.0006
Sn	0.0203	0.0188	0.0101	0.0120	0.0032	0.0059	0.0055	0.0027	0.0084	0.0031	0.0162	0.0100	0.0154	0.0049	0.0113	0.0076	0.0026	0.0081	0.0012
Sb	0.0049	0.0027	0.0009	0.0067	0.0002	0.0007	0.0003	0.0003	0.0017	0.0006	0.0039	0.0014	0.0087	0.0004	0.0009	0.0021	0.0005	0.0012	0.0005
Ba	0.0170	0.0081	0.0031	0.0101	0.0115	0.0060	0.0045	0.0002	0.0160	0.0094	0.0068	0.0024	0.0108	0.0205	0.0119	0.0056	0.0005	0.0139	0.0087
La	0.0087	0.0081	0.0034	0.0132	0.0000	0.0000	0.0042	0.0009	0.0126	0.0025	0.0082	0.0040	0.0165	0.0000	0.0000	0.0061	0.0014	0.0107	0.0026
Au	0.0005	0.0006	0.0000	0.0000	0.0002	0.0001	0.0000	0.0002	0.0000	0.0000	0.0002	0.0001	0.0000	0.0001	0.0002	0.0001	0.0002	0.0000	0.0001
Hg	0.0002	0.0003	0.0000	0.0000	0.0000	0.0000	0.0000	0.0000	0.0000	0.0000	0.0001	0.0000	0.0000	0.0000	0.0000	0.0000	0.0000	0.0000	0.0000
Tl	0.0001	0.0001	0.0001	0.0000	0.0000	0.0000	0.0001	0.0000	0.0000	0.0000	0.0000	0.0001	0.0000	0.0000	0.0000	0.0001	0.0000	0.0001	0.0000
Pb	0.0726	0.0498	0.0406	0.0599	0.0346	0.0374	0.0312	0.0182	0.0163	0.0182	0.0624	0.0437	0.0671	0.0384	0.0428	0.0356	0.0210	0.0205	0.0184
U	0.0002	0.0011	0.0007	0.0038	0.0001	0.0000	0.0000	0.0001	0.0000	0.0002	0.0017	0.0007	0.0035	0.0000	0.0000	0.0001	0.0002	0.0000	0.0000

	KC	
	2016	2017
Teflon Mass	20.74	22.08
Quartz Mass	22.11	23.91
Cl^-	0.072	0.087
NO_3^-	0.61	0.70
SO_4^{2-}	6.56	6.51
NH_4^+	2.42	2.29
Na^+	0.29	0.39
K^+	0.22	0.23
OC	5.17	5.14
EC	2.60	2.28
TC	7.78	7.42
Al	0.1243	0.1439
Si	0.1905	0.2602
P	0.0030	0.0025
S	2.5521	2.5774
Cl	0.0518	0.1088
K	0.2426	0.2929
Ca	0.0842	0.1331
Ti	0.0076	0.0096
V	0.0252	0.0198
Cr	0.0002	0.0029
Mn	0.0065	0.0118
Fe	0.1715	0.2115
Co	0.0002	0.0001
Ni	0.0062	0.0054
Cu	0.0162	0.0175
Zn	0.0764	0.0832
Ga	0.0000	0.0001
As	0.0002	0.0004
Se	0.0000	0.0000
Br	0.0053	0.0099
Rb	0.0005	0.0004
Sr	0.0009	0.0009
Y	0.0001	0.0000
Zr	0.0001	0.0010
Mo	0.0014	0.0000
Pd	0.0007	0.0000
Ag	0.0002	0.0000
Cd	0.0001	0.0003
In	0.0005	0.0006
Sn	0.0041	0.0029
Sb	0.0010	0.0000
Ba	0.0208	0.0132
La	0.0164	0.0005
Au	0.0000	0.0000
Hg	0.0000	0.0000
Tl	0.0000	0.0000
Pb	0.0156	0.0180
U	0.0000	0.0001